SOLID STATE NMR STUDY OF THE INTERFACIAL REGION IN SURFACE MODIFIED SILICA-POLY(METHYL METHACRYLATE) COMPOSITES

By

JOSEPH ROYCHEN

Bachelor of Science
Sardar Patel University
Gujarat, India
1986

Master of Science (Chemistry)
Sardar Patel University
Gujarat, India
1988

Doctor of Philosophy (Chemistry)
M. S. University
Baroda, India
1992

Submitted to the Faculty of the
Graduate College of the
Oklahoma State University
in partial fulfillment of
the requirements for
the degree of
MASTER OF SCIENCE
July, 1995

SOLID STATE NMR STUDY OF THE INTERFACIAL REGION IN SURFACE MODIFIED SILICA-POLY(METHYL METHACRYLATE) COMPOSITES

Thesis Approved:

Warren T. Ford

Thesis Adviser

K D Berlin

C L Cyr

Thomas C. Collins

Dean of the Graduate College

PREFACE

Polymer composites are high strength materials made by mixing inorganic fillers nto a polymer matrix. The physical and mechanical properties of composite materials are governed by the adhesion between the two phases. A variety of chemical and physical interactions occurring at the interface is responsible for the inherent properties of these materials. Hence, there is a need to understand the interface of the composite materials.

Uniform mixing between the components is necessary to achieve the optimum properties. Research in our lab focuses on the preparation of optically transparent composites by incorporating nanometer size particles of colloidal silica into poly(methyl methacrylate) (PMMA, a commodity plastic). The adhesion between the components can be increased by anchoring on the filler a reactive group, which is also compatible with the polymer. In silicate systems the compounds used to bond the silica to the polymer are called silane coupling agents. We used the silane coupling agent 3-(trimethoxysilyl)propyl methacrylate (TPM) to improve the adhesion between the components-a molecular glue that bonds silica to PMMA.

NMR spectroscopy is the only technique available to determine molecular structure of an amorphous solid such as the composite. The material is exposed to a strong magnetic field to probe nuclei situated in different environments within the sample. NMR can be used to determine both the molecular structure and molecular mobility within the composite. We found that the composite components were intimately mixed at the molecular level, and the presence of TPM silica does not increase rigidity of PMMA in the composite. This lays the ground work for further studies on these composites to elucidate the chemical interactions that occur at the interface of these materials.

ACKNOWLEDGMENTS

I would like to express deep appreciation to my research advisor, Professor Warren T. Ford for his guidance, instruction, valuable suggestions and his strong interest in the progress of my research. I wish to express my sincere gratitude to him for providing me with excellent research facilities and support. I am also grateful to Dr. Darrell Berlin and Dr. Corina Czekaj for serving on my graduate committee.

I would also like to thank Dr. Shanmin Zhang for his instruction and guidance in using the solids NMR and Dr. Hari Babu Sunkara for his help with the colloidal silica preparation. Many thanks to all the members of our research group for their help and friendship.

Finally, I would like to acknowledge the Department of Chemistry for giving me an opportunity to continue my education and also the generous financial support in the form of teaching assistantship during the course of my graduate study at Oklahoma State University.

Special thanks to my wife, Nurzy, for her love, support and encouragement.

TABLE OF CONTENTS

LIST OF TABLES

Chapter II

Chapter III

LIST OF FIGURES

Chapter III

LIST OF SCHEMES

Chapter I

Chapter II

PREFACE

Polymer composites are high strength materials made by mixing inorganic fillers into a polymer matrix. The physical and mechanical properties of composite materials are governed by the adhesion between the two phases. A variety of chemical and physical interactions occurring at the interface is responsible for the inherent properties of these materials. Hence, there is a need to understand the interface of the composite materials.

Uniform mixing between the components is necessary to achieve the optimum properties. Research in our lab focuses on the preparation of optically transparent composites by incorporating nanometer size particles of colloidal silica into poly(methyl methacrylate) (PMMA, a commodity plastic). The adhesion between the components can be increased by anchoring on the filler a reactive group, which is also compatible with the polymer. In silicate systems the compounds used to bond the silica to the polymer are called silane coupling agents. We used the silane coupling agent 3-(trimethoxysilyl)propyl methacrylate (TPM) to improve the adhesion between the components-a molecular glue that bonds silica to PMMA.

NMR spectroscopy is the only technique available to determine molecular structure of an amorphous solid such as the composite. The material is exposed to a strong magnetic field to probe nuclei situated in different environments within the sample. NMR can be used to determine both the molecular structure and molecular mobility within the composite. We found that the composite components were intimately mixed at the molecular level, and the presence of TPM silica does not increase rigidity of PMMA in the composite. This lays the ground work for further studies on these composites to elucidate the chemical interactions that occur at the interface of these materials.

CHAPTER 1

INTRODUCTION

COMPOSITES

The quest for preparing better materials by combining different species is gaining importance in this era of advanced technology. The growth of research in the development of composite materials is evident from the plethora of publications in the last decade. Polymeric materials can be strengthened by adding reinforcement to them in the form of particles or fibers.[1] Composites with exceptional mechanical properties have been prepared by aligning strong fibrous carbon in polymer matrices. The structure of the interface plays a significant role in the determination of the bulk properties of these materials. Several researchers[2,3] have focused their attention on understanding the interfacial properties of these materials employing various techniques.

The properties of composite materials are greatly influenced by the degree of mixing between the two phases.[4] Composites with a high degree of mixing have been achieved through the use of the sol-gel process. The application of sol-gel process to the formation of optically transparent organic-inorganic composite materials has received a great deal of attention in the recent years.[5-8] The sol-gel process involves the hydrolysis and condensation of tetraalkyl orthosilicates in the presence of a cosolvent to form three dimensional SiO_2 networks as solvent swollen gels (Scheme 1).

Numerous reports[9-16] have appeared on the preparation of organic-inorganic composites by *in situ* polymerization of metal alkoxides in organic polymers. This method has its limitations due to the low solubility of polymers in the tri-component sol-gel solution and the shrinkage associated with their drying. The shrinkage introduces considerable stress within the dried glasses, thereby preventing molding applications.[10]

Scheme 1. The Sol-Gel Process

Hydrolysis

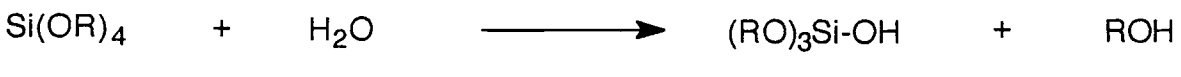

Condensation

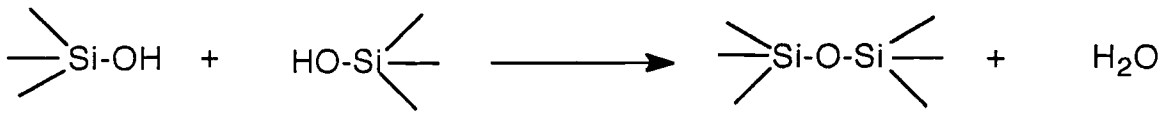

and/or

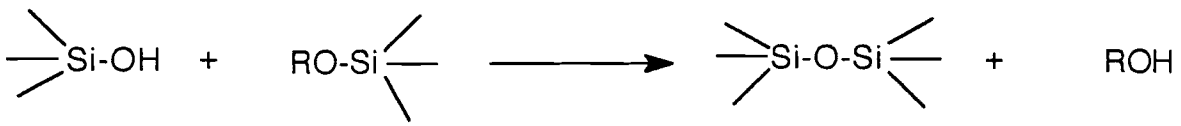

Net Reaction

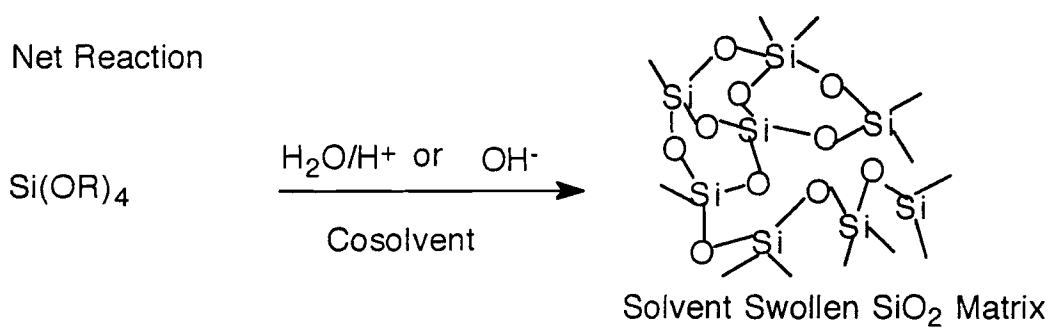

The nature and the structure of the inorganic oxide generated by hydrolysis and condensation of metal alkoxide can be controlled by such variables as pH, the amount of water added for hydrolysis, and the type of solvent employed.[17] In the cases of poly(vinyl acetate)[14] and poly(methyl methacrylate) (PMMA),[4,18] extensive hydrogen bonding was found between the silanols of the silicate network and the carbonyl groups on the polymer. These interactions retard the phase separation between the polymer and the silicate network and thus yield a continuous phase. In another approach the organic and the inorganic phases were simultaneously formed through the polymerization of the

organic monomer and inorganic precursors.[16] The structure of the organic and the inorganic components, the phase morphology, the degree of interpenetration, and the nature of the bonds between the phases control the properties of such composites.

PMMA/SiO_2 composites have been previously prepared by impregnating porous SiO_2 networks with PMMA.[9] This was achieved by immersing pre-dried, porous sol-gel xerogels into methyl methacrylate, and then allowing the monomer to polymerize within and around the inorganic network. Introducing covalent bonds between the phases by pretreating the xerogel with 3-(trimethoxysilyl)propyl methacrylate (TPM) has been found to improve the optical clarity and increase the modulus of rupture. The process is outlined in Scheme 2.

Scheme 2. Surface Modification of Colloidal Silica and Composite Preparation

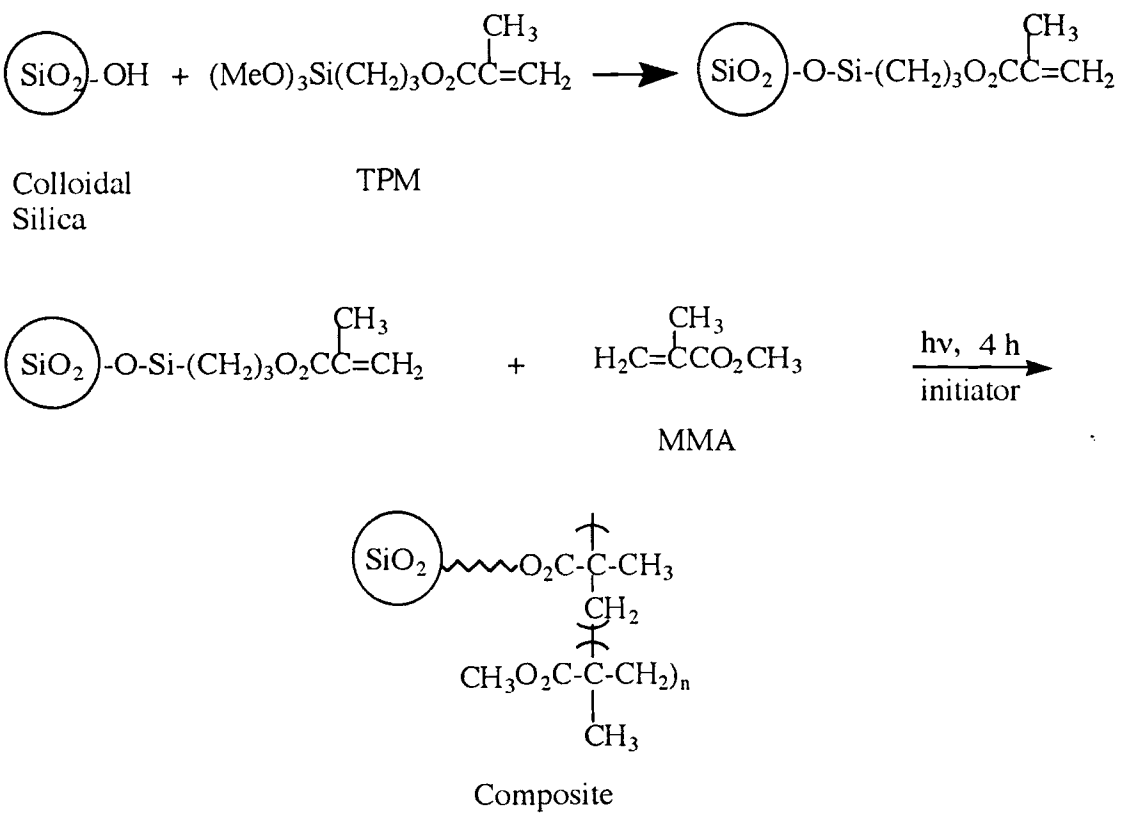

Landry and co-workers[4,12] suggested that the polymers which result in optically transparent composites with tetraethyl orthosilicate (TEOS) are those capable of H bond formation, with residual hydroxyls present on the surface of SiO_2 formed under basic conditions. Infrared studies revealed a weakly hydrolyzed silicate intermediate with a large amount of unreacted TEOS. The films apparently phase separated into TEOS rich and PMMA rich domains with weak interactions between them. They reported that the base-catalyzed condensed gels had more $\underline{Si}(OSi)_4$ (Q^4) sites than those formed under acidic conditions. We also found a large fraction of Q^4 sites in our samples from quantitative solid NMR studies of samples prepared by the base-catalyzed reaction.

SOLIDS NMR

A wide variety of NMR experiments can be applied to probe the structure and dynamics of the interface and the bulk material.[19-21] The chemical shift provides information about the molecular environment of a particular nucleus.[22] The difference in the resonance frequencies of a particular nucleus in the sample from a reference nucleus is called the chemical shift. In solids, the molecules may be oriented in all possible directions with respect to the applied field B_o, and this results in a spread of chemical shifts called the chemical shift anisotropy (CSA). The chemical shift in each orientation is proportional to $3(\cos^2\phi - 1)$, where ϕ is the angle between the magnetic field and the principal axis about which the chemical shift is defined. Since CSA is a shielding effect proportional to the applied field, the measurement of the shielding tensors along specific molecular directions can yield useful structural information, such as the electronic charge distribution in that direction.[23] Knowledge of the shielding tensors is valuable for the characterization of motions by variable temperature studies.

The motion of distinct regions in a filled systems like composites can be analyzed by line shape analysis. Such studies have provided detailed information about filled

elastomeric systems. Broader lines are associated with amorphous or cross-linked regions, and the narrow lines represent crystalline or mobile regions in a material. Variable temperature studies can distinguish between the two.[24]

When a nucleus is placed in an external magnetic field, it experiences not only the external field but also the local fields from the neighboring nuclei (B_{loc}). The local field experienced by two nuclei is given by the equation[22]

$$B_{loc} = (\pm)\ \mu\ (3\ \cos^2\theta - 1)/r^3$$

where r is the distance between the two nuclei, and θ is the angle which the vector connecting the two nuclei makes with the external field. The + (parallel) and the - (anti parallel) sign reflect the spin alignment of the neighboring nucleus with respect to the applied field B_o, and μ is the magnetic moment.

The resonance lines in the solids spectrum are broadened by the anisotropic dipole-dipole interactions discussed above and by chemical shift anisotropy. By spinning the sample at kHz frequencies at the "magic angle" ($\theta = 54.74^o$), the ($3\ \cos^2\theta - 1$) term becomes zero, attenuating the contributions from the homonuclear dipolar broadening and chemical shift anisotropy. The combination of techniques of high power proton decoupling, fast magic-angle spinning, and cross polarization of proton spin to the other nuclei of lower abundance can produce a high resolution spectrum.

Another factor is the very long spin lattice relaxation time T_1 in solids, which demands longer delay periods between pulses for the nuclei to relax fully to the original equilibrium state of magnetization. This restricts the number of scans that could be accumulated in order to obtain a good spectrum. The problem of long relaxation times in solids can be overcome by utilizing the cross polarization (CP) technique. In a cross polarization experiment, a strong coupling between the nuclei is achieved resulting in a significant increase in the signal of the low naturally abundant nucleus. This condition is

called the Hartmann-Hahn match condition, which can be attained by adjusting the value of the applied field so that an abundant nucleus ^{1}H and the other nucleus (^{13}C, ^{29}Si, ^{31}P etc.) have the same Larmor frequency in the rotating frame, i.e., $\omega_{1H} = \omega_{13C}$. This allows the measurement of the dynamic parameters T_1 and $T_{1\rho}$, the spin lattice relaxation time and the spin lattice relaxation time in the rotating frame, respectively, through the less abundant nucleus. T_1 is sensitive to motions near the Larmor (resonance) frequency, 4-600 MHz, while $T_{1\rho}$ is sensitive to motions in the 10-60 kHz region.[21] Therefore, $T_{1\rho}$ measurements can be used to probe molecular motions that are orders of magnitude slower than those studied by conventional T_1 measurements. Detailed information about the intermolecular interactions and morphology can be obtained by examining the relaxation times T_1, $T_{1\rho}$, and T_2 (spin-spin relaxation time) of various nuclei in a composite sample.

Several silica-polymer composites have been analyzed by ^{13}C and ^{29}Si solid NMR spectroscopy. Zumbulayadis and O'Reilly[25] found that the cross-polarization time constant T_{SiH} for ^{1}H to ^{29}Si was shorter for the silica-poly(vinyl alcohol) (PVA) composites than for the silica alone. This was interpreted as being due to the PVA making the surface hydroxyls more rigid and hence more effective at cross-polarizing silica. Deuteration of the exchangeable protons (surface and alcohol hydroxyls) resulted in a slower, but measurable T_{SiH}. This showed that even the backbone PVA protons could effectively cross-polarize the surface silicones. They concluded that this was a tightly coupled spin system.

Weeding and co-workers[26,27] examined the composites made from nylon-6 and glass using the ^{13}C chemical shift data. A comparison of bulk and glass-filled (including surface treated glass) composites showed that a greater amount of γ-crystalline form of nylon-6 was produced when the composite was processed as compared with the original

bulk polymer. In the absence of the glass spheres, the γ form reverted back to the α form. An amorphous polymer layer was found to be intimately associated with the glass.

Pioneering work by Maciel's group since 1980 has been done on silica gel to analyze the surface properties.[28-37] Employing the CPMAS technique (^{29}Si NMR) they identified the various silicon sites as Q^2 (-90.6 ppm), Q^3(-99.8 ppm), and Q^4(-109.3 ppm) for the geminal, single silanol and siloxane linkages, respectively, in a commercial silica gel sample. They are as represented below in Scheme 3.

Scheme 3. Various Silicon Sites in a Silica Sample

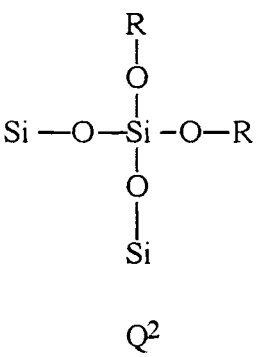

Q^2

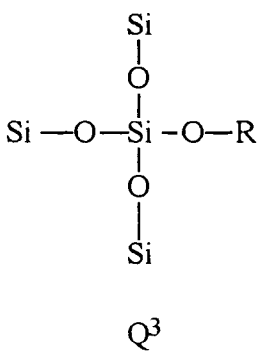

Q^3

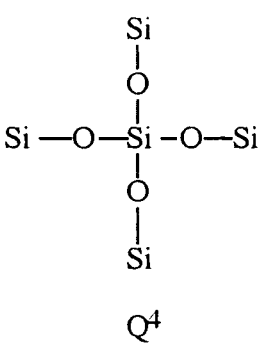

Q^4

R = OH/OCH_2CH_3

In another study,[38] they developed methodology which provides quantitative relationships on structure and reactivity from ^{29}Si CPMAS spectra of various silica gels and surface modified silica gels. Geminal-hydroxyl silanol sites were found to be more reactive to hexamethyldisilazane than lone silanol sites. Motional dynamics in a long

chain aliphatic phase bonded to silica gel were studied by ^{13}C CPMAS relaxation measurements.[33] Differences in cross-polarization rates and proton $T_{1\rho}$ and T_1 values observed for samples prepared by silylation of silica gel with dimethyloctadecylchlorosilane (DMODCS) and dimethyloctylchlorosilane (DMOCS) identified methyl group rotation as a likely principal source of proton spin-lattice relaxation. Cross-polarization efficiency was observed to decrease with increasing distance from the surface along the alkyl chain.

Different ^{29}Si CPMAS NMR pulse sequences have been used to study the effects of ^1H spin reservoirs on silica gel surface.[28,37] Both ^1H-^{29}Si dipolar-dephasing experiments and proton-coupled ^{29}Si CPMAS results indicate that various hydroxyl groups of silanols in silica gel undergo rapid ^1H spin exchange, and that the most strongly coupled protons provide the dominant source of cross-polarization to geminal-silanol silicon atoms. ^1H-^1H dipolar dephasing prior to ^1H-^{29}Si cross-polarization shows a rapid ^1H spin exchange between ^1H reservoirs of single silanol groups and of geminal silanol groups. A slower ^1H-^1H dipolar-dephasing decay due to proton spin exchanges was found for the ^1H spin reservoirs of single silanol groups.

The CRAMPS (combined rotation and multiple-pulse spectroscopy) technique has been used to obtain high-resolution ^1H NMR spectra of silica gel samples at different stages of hydration.[34] The silica gel sample (S-679, Fisher) had resolvable peaks for physisorbed water and for two distinguishable types of silanol protons. Spin-lattice relaxation, dipolar dephasing, and spin exchange provided evidence that both types of silanol protons are physically proximate to each other on the surface.

The major goal of this work is to study the interface of the 3-(trimethoxysilyl)-propyl methacrylate (TPM) coated colloidal silica-poly(methyl methacrylate) composites by the versatile solid NMR spectroscopy.

References

(1) Manson, J, A.; Sperling, L. H. *Polymer Blends and Composites*, Plenum: New York, 1976.

(2) Hergeth, W-D.; Steinau, U-J.; Bittrich, H-J.; Simon, G.; Schmutzler, K. *Polymer* **1989**, *30*, 254.

(3) Carlier, E.; Guyot, A.; Revillion, A.; Darricades, M. F.; Petiaud, R. *Reactive Polymers* **1991**, *16*, 41.

(4) Landry, C. J. T.; Coltrain, B. K.; Wesson, J. A.; Lippert, J. L.; Zumbulyadis, N. *Polymer* **1992**, *33*, 1496.

(5) Brinker, C. J.; Scherer, G. W.; *Sol-gel Science*, Academic, New York, 1990.

(6) Ellsworth, M. W.; Novak, B. M. *Chem. Mater.* **1993**, *5*, 839.

(7) Wei, Y.; Bakthavatchalam, R.; Yang, D.; Whitecar, C. K. *Polym. Prepr. (Am. Chem. Soc., Div. Polym. Chem.)* **1991**, *32*, 503.

(8) Wei, Y.; Bakthavatchalam, R.; Yang, D.; Whitecar, C. K. *Chem. Mater.* **1990**, *2*, 337.

(9) Pope, E. J. A.; Asami, M.; Mackenzie, J. D. *J. Mater. Res.* **1989**, *4*, 1018.

(10) Huang, H. H.; Orler, B.; Wilkes, G. L. *Macromolecules* **1987**, *20*, 1322.

(11) Novak, B. M.; Davies, C. *Macromolecules* **1991**, *24*, 5481.

(12) Landry, C. J. T.; Coltrain, B. K.; Landry, M. R.; Fitzgerald, J. J.; Long, V. K. *Macromolecules* **1993**, *26*, 3702.

(13) Fitzgerald, J. J.; Landry, C. J. T.; Schillace, R. V.; Pochan, J. M. *Polym. Prepr. (Am. Chem. Soc., Div. Polym. Chem.)* **1991**, *32*, 532

(14) Fitzgerald, J. J.; Landry, C. J. T.; Pochan, J. M. *Macromolecules* **1992**, *25*, 3715.

(15) Ellsworth, M. W.; Novak, B. M. *J. Am. Chem. Soc.* **1991**, *113*, 2756.

(16) Novak, B. M. *Adv. Mater.* **1993**, *5*, 422.

(17) Brinker, C. J. *J. Non-Cryst. Solids* **1988**, *100*, 31.

(18) Landry, C. J. T.; Coltrain, B. K.; Brady, B. K. *Polymer* **1992**, *33*, 1486.

(19) Fyfe, C. A. *Solid State NMR for Chemists*, CFC Press, Guelph, Ontario, 1983.

(20) Schaefer, J.; Stejskal, E. O. *J. Am. Chem. Soc.* **1976**, *98*, 1031.

(21) Segre, A. L.; Capitani, D. *Trends in Polymers* **1993**, *1*, 280.

(22) Rahman, A. *Nuclear Magnetic Resonance*; Springer-Verlag: New York, 1986.

(23) Yannoni, C. S. *Acc. Chem. Res.* **1982**, *15*, 201.

(24) McBrierty, V. J.; Douglass, D. C. *J. Polym. Sci. Macromol. Rev.* **1981**, *16*, 295.

(25) Zumbulayadis, N.; O'Reilly, J. M. *Macromolecules* **1991**, *24*, 5294.

(26) Weeding, T. L.; Veeman, W. S.; Angad Gaur, H.; Huysmans, W. G. B. *Macromolecules* **1988**, *21*, 2028.

(27) Weeding, T. L.; Veeman, W. S.; Jenneskens, L. W.; Angad Gaur, H.; Schuurs, H. E. C.; Huysmans, W. G. B. *Macromolecules* **1989**, *22*, 706.

(28) Chuang, I-S.; Kinney, D. R.; Maciel, G. E. *J. Am.. Chem. Soc.* **1993**, 115, 8695.

(29) Maciel, G. E.; Sindorf, D. W.; Bartuska, V. J. *J. Chromatogr.* **1981**, 205, 438.

(30) Sindorf, D. W.; Maciel, G. E. *J. Am. Chem. Soc.* **1981**, *103*, 4263.

(31) Sindorf, D. W.; Maciel, G. E. *J. Am. Chem. Soc.* **1983**, *105*, 3767.

(32) Sindorf, D. W.; Maciel, G. E. *J. Phys. Chem.* **1983**, *87*, 5516.

(33) Sindorf, D. W.; Maciel, G. E. *J. Am. Chem. Soc.* **1983**, *105*, 1848.

(34) Maciel, G. E.; Sindorf, D. W. *J. Am. Chem. Soc.* **1980**, *102*, 7606.

(35) Sindorf, D. W.; Maciel, G. E. *J. Am. Chem. Soc.* **1983**, *105*, 1487.

(36) Bronnimann, C. E.; Zeigler, R. C.; Maciel, G. E. *J. Am. Chem. Soc.* **1988**, *110*, 2023.

(37) Chuang, I-S.; Kinney, D. R.; Bronnimann, C. E.; Ziegler, R. C.; Maciel, G. E. *J. Phys. Chem.* **1992**, *96*, 4027.

(38) Kinney, D. R.; Chuang, I-S.; Maciel, G. E. *J. Am. Chem. Soc.* **1993**, *115*, 6786.

(39) Sindorf, D. W.; Maciel, G. E. *J. Phys. Chem.* **1982**, *86*, 5208.

CHAPTER 2

COMPOSITE PREPARATION

Introduction

Composite materials consisting of organic polymers and inorganic particles or fibers are utilized in numerous applications. A critical challenge in the design of these composites is to control the mixing between the two chemically dissimilar phases. Silane coupling agents have been found to improve the adhesion between these phases.[1] Silane coupling agents generally are organo-functional silanes of the type X_3SiRY where Y is a non-hydrolyzable organic group and X is a hydrolyzable group such as halide or alkoxide. Cross-reaction of the organic and inorganic components retards phase separation leading to the production of hybrid materials.

The properties of composite materials are greatly influenced by the degree of mixing between the two phases. Composites with a high degree of mixing have been achieved through the sol-gel process. Several workers[2-6] have reported the preparation of transparent composites with improved mechanical properties by polymerization of TEOS in the presence of polymers by the sol-gel process. The use of silane coupling agents in the sol-gel process enhances the mixing by forming covalent bonds between the phases. Another approach involved simultaneous polymerization of inorganic and organic monomers as reported by Novak and co-workers[7, 8] in producing homogeneous composites.

Composites have been prepared in our lab[9] with surface modified colloidal silica (152 nm particles) dispersed in MMA monomer and then polymerized with a photo initiator. The composite films were transparent and iridescent. We have used the silane coupling agent 3-(trimethoxysilyl)propyl methacrylate (TPM) for the coating of the silica.

This substance reacts rapidly under mild conditions with the silica surface and introduces covalent bonds between the phases, thereby improving the optical and mechanical properties of the system.[10] The colloidal silica particles do not aggregate further during the procedure for coating, which forms in an organic layer of few nanometers thick on the surface.

This chapter describes the preparation of colloidal silica particles, their surface modification with the silane coupling agent, and the preparation of TPM silica-MMA composites. A preliminary ^{29}Si solids NMR study on composites prepared with 152 nm TPM silica particles revealed too few Si sites from the surface modifier. Hence, smaller particles of 9 nm were prepared and used in making the composites.

Experimental

Materials. Tetraethyl orthosilicate (TEOS, Aldrich) was distilled under reduced pressure prior to use. Absolute ethanol (Aaper) was freshly distilled. Ammonium hydroxide (Baker) was used as received. 3-(Trimethoxysilyl)propyl methacrylate (TPM, Aldrich) was distilled under reduced pressure at 104 °C. 2,2-Dimethoxy-2-phenyl acetophenone (DMPA, Aldrich) was used as received. Methyl methacrylate (MMA, Aldrich) was freshly distilled under reduced pressure at 40 °C.

Colloidal silica. Colloidal silica dispersion in aqueous ammoniacal ethanol was prepared by the Stöber method.[11,12] A 5 L round bottomed flask was charged with 75 mL of NH_4OH, and 3450 mL of absolute ethanol. TEOS (150 mL; 0.2 M) was added rapidly to the magnetically stirred mixture at 22 °C. The reaction was run for 10 hours, to obtain the colloidal silica dispersion.

TPM Silica. TPM-coated silica particles were prepared according to the procedure described by Philipse and Vrij.[13] To a 2.0 L silica dispersion (30.4 g of silica)

was added 150 mL of TPM, and the mixture was stirred for 2.5 hours at room temperature (24 °C). The final volume of the mixture was reduced to 750 mL by slowly distilling off ethanol at 32 °C under reduced pressure over a period of 7.5 hours.

Purification of the colloidal dispersion. The dialysis tubing made from regenerated cellulose (Spectra/Por® 7) was thoroughly washed with distilled water and with absolute ethanol several times. The tube was tied at one end and the colloidal dispersion was (30 mL) was transferred into it. This was then suspended into methanol in a 1000 mL measuring cylinder to the level of the colloidal particles. Methanol was stirred using a magnetic stirrer and several times exchanged with fresh methanol over a period of 2 days until the ethanol was completely removed from the colloidal dispersion. This was checked via the proton NMR spectrum of the dispersion. The dialysis also removes the unbound TPM from the colloidal dispersion. The TPM-coated silica dispersion was further concentrated to about 75 mL under vacuum to get a solids content of 10.6 weight percent. Using a similar dialysis procedure, these particles were transferred from methanol into methyl methacrylate monomer.

The colloidal dispersion in methyl methacrylate was concentrated to obtain a solids content of about 50%. This was done by evaporating the dispersion in a beaker with stirring and bubbling of a slow stream of argon gas. The concentrated dispersion was then used to prepare the composite films. Solids content was determined by placing 250-500 μL of the dispersion in a petri dish, evaporating the solvent in a glove bag, and then heating at 120 °C for 3-4 hours to constant weight of the residue.

Photochemical cell. This cell was made using three teflon spacers of thickness 132 μm each sandwiched between two rectangular glass slides (3" x 2" x 1" mm). Three sides of the glass cells were sealed with epoxy at room temperature (Devcon, 5 Minute Epoxy, Devcon Corporation, IL), and the teflon spacers were removed. After filling with the sample for polymerization, the fourth side was also sealed and cured at room

temperature for about 5 minutes before mounting the cell onto the photochemical reaction assembly.

Photopolymerization. About 2 mL of the colloidal dispersion in MMA was added to the photoinitiator DMPA (1% by weight of the monomer) in a small silylated glass vial. The solution was mixed well by shaking and then purged with N_2 gas for a minute before injecting into the photochemical cell. After curing the epoxy seal, the cell was placed vertically at a distance of 7.9 cm from the UV source (450 W medium pressure mercury lamp) in the photochemical reactor unit. The lamp was cooled by circulating water in a quartz immersion jacket. The reaction was stopped after 4 hours, and the cell was cut open to remove the polymer film. About 9.65 g of the composite was prepared from 6 repetitions. Preliminary photopolymerization reactions with methyl methacrylate showed that the reaction was complete in 4 hours.

Analytical Methods. Solution ^{13}C NMR spectra were obtained at 101 MHz on a Varian XL-400 spectrometer.

Transmission electron microscopy was done at the OSU Electron Microscopy Laboratory on a JEOL JEM-100CX II microscope at 75 kV. One drop of the colloidal dispersion was placed on the sample grid, allowed to stand for 30-40 s, and the solvent was wicked away using filter paper. This procedure was repeated with a 3% uranyl acetate solution to stain the sample. Particle sizes were determined by measuring at least 100 particles on the photographic negative and calculating the number average and weight average diameters.

Elemental analyses were done at Atlantic Microlab Inc. The samples were prepared by evaporating about 20 mL each of the colloidal silica and TPM-coated colloidal silica dispersions to dryness in a glove bag in air and then drying in vacuum for 24 hours at 52 °C.

Results and Discussion

Colloidal silica particles of 9 nm size were prepared by hydrolysis and condensation of tetraethoxy silane according to the method developed by Stöber, Fink and Bohn.[11] Their method produces monodisperse colloidal dispersions. Several aspects of the colloidal systems prepared by their method have been the subject of various publications.[13,14] Organo-alkoxy silane in a mixture of water, ammonia and the cosolvent ethanol may undergo many different reactions. The reactions can be represented as,

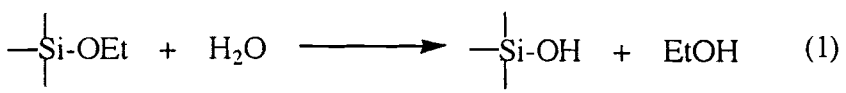

(1)

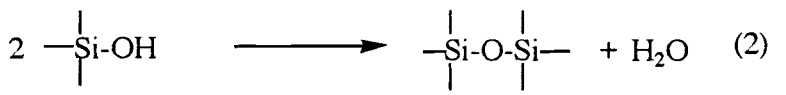

(2)

Philipse and Vrij[13] showed that it is also possible to use silane coupling agents to prepare stable, surface-coated silica dispersions. The TPM-coated colloidal silica dispersions prepared in this study by the similar procedure were also found to be stable over a long period of time. Dynamic light scattering of the dispersion gave the average diameter of the particles to be 20 nm. Light scattering is very sensitive to small amounts of larger particles like clusters, and hence, the large deviation from the TEM diameter of (10 nm).

The effect of changing the concentration of the reactants in the hydrolysis was studied extensively by Zukoski's group.[15] They developed an equation to correlate the final particle diameter in nm (d) to the concentrations of water, ammonia and tetraethyl orthosilicate (TEOS).

$$d = A[H_2O]^2 \exp(-B[H_2O]^{1/2}) \quad (1)$$

where

$$A = [TEOS]^{1/2}(82.06 - 151.3[NH_3] + 1202[NH_3]^2 - 365.8[NH_3]^3)$$

$$B = 1.051 + 0.5230[NH_3] - 0.1283[NH_3]^2$$

OR

$$d = A[H_2O]^2 \exp(-B[H_2O]) \quad (2)$$

where

$$A = [TEOS]^{-1/2}(-1.042 + 40.57[NH_3] - 9.313[NH_3]^2)$$

$$B = 0.3264 - 0.2727[TEOS]$$

Zukoski states that these equations come within 20% of the actual experimentally measured particle diameters. He formulated these equations for reactions run at 25 °C. For our system, the calculated particle diameter was found to be 12 nm and 11 nm from equations 1 and 2, respectively. The concentrations were 0.1899 M (TEOS), 0.3128 M (NH_3) and 0.7233 M (H_2O). This agrees well with the experimental value of 10 nm obtained for our system from the TEM measurement. The number average (d_n) and weight average (d_w) particle diameters were calculated from the following equations,

$$d_n = \sum n_i d_i / \sum n_i \quad (3)$$

$$d_w = (\sum n_i d_i^6 / \sum n_i d_i^3)^{1/3} \quad (4)$$

The particles were seen as distorted spheres in the TEM micrograph (Figure 1).

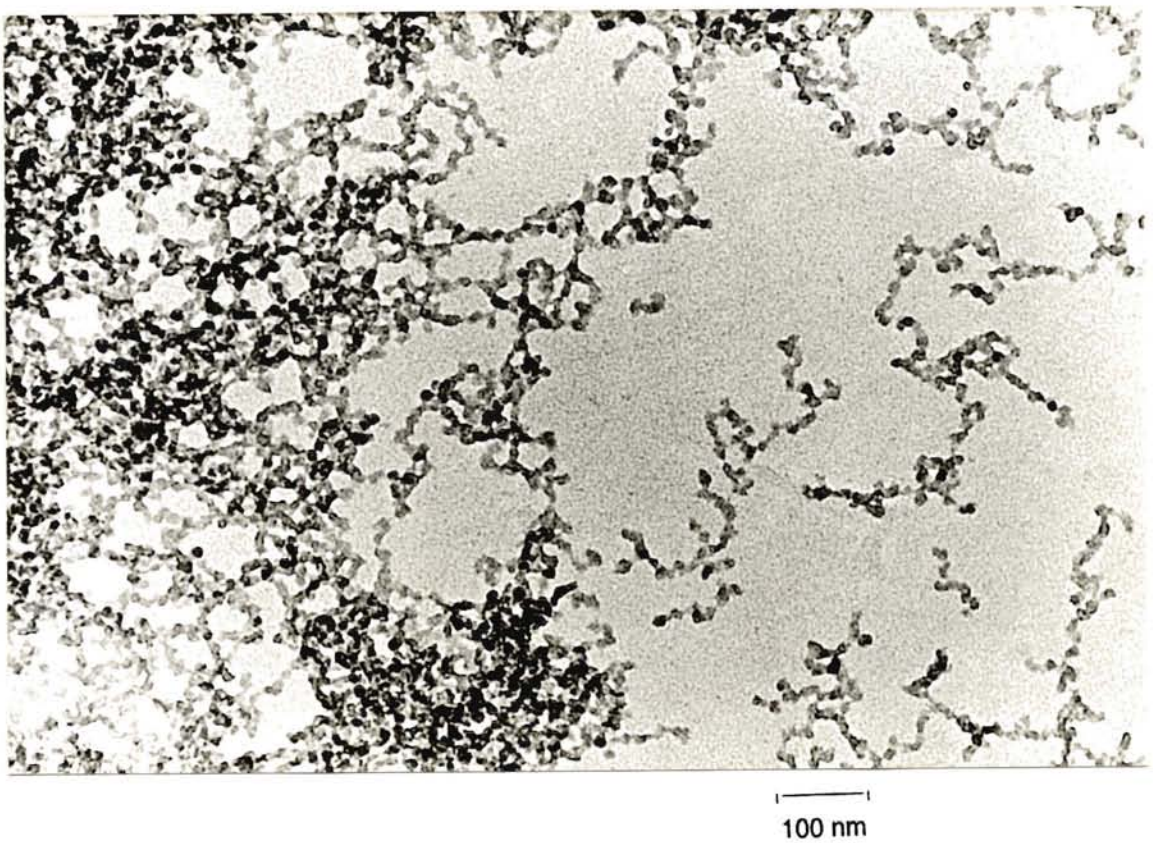

Figure 1. TEM of colloidal silica, TEM magnification 100,000.

Assink and Kay[16,17] have reported that silica formed by base catalyzed hydrolysis of TEOS contains a significant number of ethoxy groups because hydrolysis is the rate limiting step in the polymerization. The results from the elemental analysis (Table 1) also suggest the presence of ethoxy groups.

Table I. Results of Elemental Analyses

Sample	% C (mg-atom/g)	% H (mg-atom/g)
Parent Silica	2.92 (2.43)	1.96 (19.4)
TPM silica	24.30 (20.3)	3.70 (36.7)

The values in Table 1 suggest that the carbon content of TPM silica is much larger than that of the corresponding TEOS condensate, confirming the presence of TPM on the silica surface. The only source of carbon in parent silica is from the unhydrolyzed OC_2H_5 groups. The lower carbon-hydrogen ratio of the parent silica reflects the presence hydrogens from silanol and water. Higher hydrogen concentrations were also reported by Philipse and Vrij[13] on similar samples. Silanol and ethoxy groups may be distributed through the whole particle forming a loose network rather than a fully condensed network.

Dialysis was found to be an efficient method for the purification of the TPM coated silica and its transfer into the MMA monomer. The unreacted TPM diffused out into methanol over a period of two days, and TPM remaining in the dispersion was checked by ^1H or ^{13}C NMR. Transfer of the colloidal particles into the monomer MMA was complete after four solvent changes since the ^1H NMR spectrum of the dialysate did not show any peaks from methanol. The chemical structure of the TPM silica (**3**) is shown in Scheme 1.

The number of TPM monomeric units per square nanometer of silica surface can be calculated from the difference in the weight percentage of carbon before and after coating. For our sample, the difference was 21.65 wt %. The specific surface area of the sample can be calculated from the equation

$$O = 3\,(\delta r)^{-1}$$

where r is the particle radius (5.3 nm) and δ is the density. We obtained a value of 339 m^2/g for our sample by considering the density to be 1.67 g/cm^3 (density of the 152 nm diameter TPM-coated particles determined by pycnometric method in our lab[9]). Thus the coating corresponds to about 32 carbon atoms /nm^2 of the silica surface. Since the TPM unit on the surface contains eight carbons (seven from the trimethylsilyl methacrylate and

one from an OCH_3 group of the TPM residue as shown in the ^{13}C CPMAS spectrum), there are about 4 TPM units/nm^2 of the surface.

The TPM coated colloidal silica dispersion in MMA was polymerized with one weight percent of the DMPA photoinitiator. The TPM groups on the silica copolymerize with MMA, as shown in Scheme 1, to yield the composite.

Scheme 1. Synthesis of the TPM Silica-PMMA Composite.

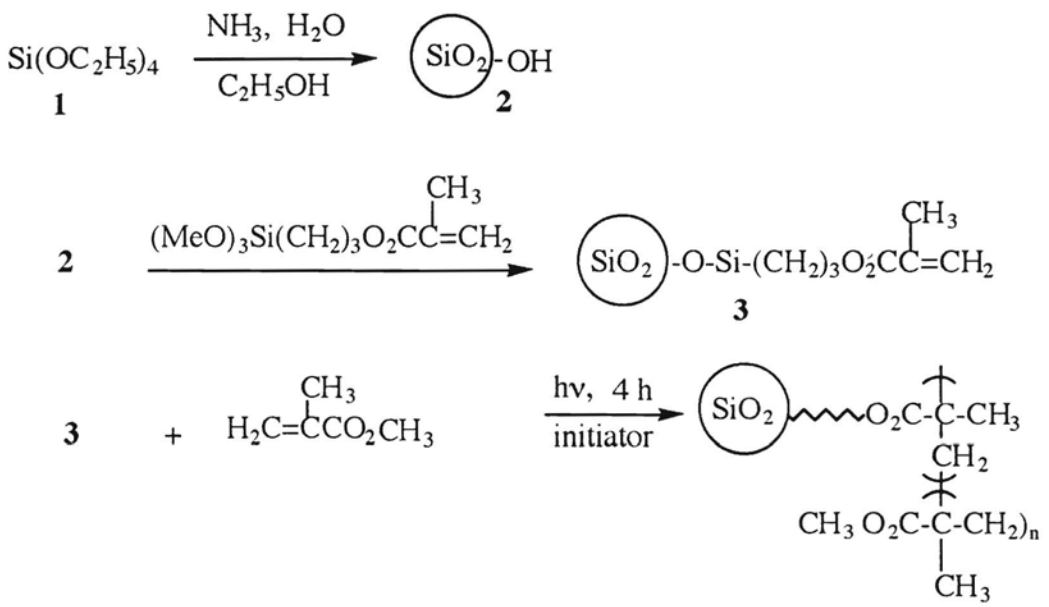

The amount of the initiator and its extinction coefficient of 247 M^{-1} cm^{-1} at λ_{max} = 336 nm indicate there should be uniform irradiation throughout the 396 μm glass cell. The polymerization was complete in 4 hours. About 50 wt % (~25 vol %) of the TPM-silica was present in the composite. The high solids content is expected to improve the sensitivity of ^{29}Si NMR spectroscopic analysis of the TPM silica-PMMA interface.

References

(1) Plueddemann, E. P. *Silane Coupling* Agents, 2nd ed.; Plenum Press: New York, 1991.

(2) Landry, C. J. T.; Coltrain, B. K.; Landry, M. R.; Fitzgerald, J. J.; Long, V. K. *Macromolecules* **1993**, *26*, 3702.

(3) Fitzgerald, J. J.; Landry, C. J. T.; Schillace, R. V.; Pochan, J. M. *Polym. Prepr. (Am. Chem. Soc., Div. Polym. Chem.)* **1991**, *32*, 532.

(4) Fitzgerald, J. J.; Landry, C. J. T.; Pochan, J. M. *Macromolecules* **1992**, *25*, 3715.

(5) Landry, C. J. T.; Coltrain, B. K.; Brady, B. K. *Polymer* **1992**, *33*, 1486.

(6) Landry, C. J. T.; Coltrain, B. K.; Wesson, J. A.; Zumbulyadis, N.; Nippert, J. L. *Polymer* **1992**, *33*, 1496.

(7) Ellsworth, M. W.; Novak, B. M. *J. Am. Chem. Soc.* **1991**, *113*, 2756.

(8) Novak, B. M.; Davies, C. *Macromolecules* **1991**, *24*, 5481.

(9) Sunkara, H. B.; Jethmalani, J. M.; Ford, W. T. *Chem. Mater.* **1994**, *6*, 362.

(10) Novak, B. M. *Adv. Mater.* **1993**, *5*, 422.

(11) Stöber, W.; Fink, A.; Bohn, E. *J. Colloid Interface Sci.* **1968**, *26*, 62.

(12) Badley, R. D.; Ford, W. T.; McEnroe, F. J.; Assink, R. A. *Langmuir* **1990**, *6*, 792.

(13) Philipse, A. P.; Vrij, A. *J. Colloid Interface Sci.* **1989**, *128*, 121.

(14) Van Blaaderen, A.; Ph. D. Thesis, University of Utrecht, *Colloidal Dispersions of (Organo-) Silica Spheres: Formation Mechanism, Structure and Dynamics*, 1992.

(15) Bogush, G. H.; Tracy, M. A.; Zukoski, C. F. *J. Non. Cryst. Solids* **1988**, *104*, 95.

(16) Assink, R. A.; Kay, B. D. *Mat. Res. Res. Soc. Symp. Proc.* **1984**, *32*, 301.

(17) Kay, B. D.; Assink, R. A. *Mat. Res. Res. Soc. Symp. Proc.* **1986**, *73*, 157.

CHAPTER 3

SOLID STATE NMR STUDY

Introduction

The unique surface properties of silica make it a versatile material in numerous applications.[1] ^{13}C and ^{29}Si solid state NMR analysis with cross polarization (CP) and magic-angle spinning (MAS) has been used to obtain valuable information regarding the structures of carbon and silicon sites present on the parent silica, composite, and the colloidal silica surfaces. Theoretically, CP from H to X enhances the X NMR signal compared with direct polarization by the ratio γ_H/γ_X of the magnetogyric ratios. More scans can be accumulated in the same measurement time owing to shorter relaxation time of the protons than of the X nuclei. This allows detailed study of structures and transformations at the silica surface.

The major goal of this NMR study is to obtain specific information on the structure and dynamics of the interfacial material and to identify differences from material in the bulk phase. Extensive studies have been performed on commercial and modified silica gel samples by Maciel's group.[2-11] They observed three types of protons distinguishable via their spin dynamic interactions with Si atoms: hydrogen bonded Si-OH that have large homonuclear and heteronuclear dipolar couplings; non hydrogen bonded Si-OH that have weak homonuclear and strong heteronuclear dipolar couplings; and adsorbed water that is weakly dipolar coupled.[10] These were detected by ^1H CRAMPS (Combined Rotation and Multiple Pulse Spectroscopy) experiments and by differences in their dipolar interactions with other protons and ^{29}Si nuclei.

Our samples have more complicated surface structures than the silica gels studied earlier because of the residual ethoxy groups from the preparative process, the TPM

interface and the PMMA matrix. The aim of this work is to analyze the structures of the interfaces of colloidal silica, TPM-modified silica, and the composite by a variety of dynamic CPMAS experiments and to identify the set of protons in each sample that communicate by spin diffusion and that cross-polarize to ^{13}C and ^{29}Si atoms. The spin dynamic experiments depend on the strengths of dipolar interactions in the solid described by[12]

$$B_{loc} = h\,\gamma_H(3\cos^2\theta-1)/4\pi r^3 \qquad (1)$$

where B_{loc} is the local magnetic field at a nucleus due to a neighboring magnetic nucleus having magnetogyric ratio γ_H, r is the internuclear distance, θ is the angle between the internuclear vector and the primary magnetic field B_o, and h is Planck's constant.

Experimental Section

The ^{13}C solid NMR spectra were recorded on a Chemagnetics CMX-300 spectrometer at 75.7 MHz equipped with an auxiliary high power amplifier and solid state probes using 5 mm and 7.5 mm rotors with magic angle spinning capability. The Hartmann-Hahn conditions[13] and the magic angle were adjusted using the aromatic signal from hexamethylbenzene. Probe tuning was optimized, and the reflected power from the decoupler was minimized for each sample. Experiments were done at room temperature (19-22 °C), and the samples were packed in zirconia rotors. Typical measurement conditions were as follows: ^1H 90° pulse width, 5 μs; spinning frequency, 4 kHz; cross-polarization and decoupling frequency, 50 kHz; spectral width, 50 kHz. Chemical shifts were referred to the aromatic carbon band of hexamethylbenzene (signal at 132.2 ppm) using TMS as the external reference.

^{29}Si NMR were also obtained on the above instrument at 59.8 MHz with a proton 90° pulse width of 6 μs, corresponding to cross-polarization and decoupling frequencies of 42 kHz. The Hartmann-Hahn condition was optimized by using the narrow signal of

2-(trimethylsilyl)ethanesulfonic acid, sodium salt (signal at 1.7 ppm from TMS). Direct polarization experiments were also done with a ^{29}Si 90° pulse width of 5 μs and 200 s delay between the pulses. The spinning rate was 2 kHz for all the experiments. All samples were dried at 52 °C under vacuum for 24 hours and crushed into a fine powder before filling the rotors. Typical sample amounts were about 150-200 mg and 600-700 mg in the 5 mm and 7.5 mm rotors, respectively.

Diffuse reflectance FTIR spectroscopy (DRIFTS) were acquired with a Nicolet Magna IR 750 spectrometer with diffuse reflectance accessory. The powder samples were directly transferred into the sample cell. The spectra were acquired after 32 scans.

Results and Discussion

^{13}C CPMAS Spectra. ^{13}C CPMAS spectra for the three samples, colloidal silica, TPM-modified silica, and the TPM silica-PMMA composite were obtained by the Quasi-Adiabatic Cross-Polarization sequence (QACP) developed in our lab.[14] In this sequence, the amplitude of the RF field is varied in an ascending order on the X channel. This allows efficient proton spin transfer to the X spin under static and high speed MAS conditions. This sequence has been found to be insensitive to mismatch conditions and also advantageous in obtaining enhanced signal intensity in samples with weak signals. The pulse sequence is as shown in Figure 1.

The ^{13}C CPMAS spectrum of PMMA (Figure 2) is broad compared to that measured in solution. All five carbon resonances of PMMA can be assigned in the spectrum. The methyl carbon resonance at 18 ppm is broadened due to the dispersion of the chemical shift which results from different conformations and configurations in the solid state. The quaternary carbon resonance is at 45 ppm. The methylene carbon resonance is partially hidden under the methoxy carbon at 52 ppm and is visible as a

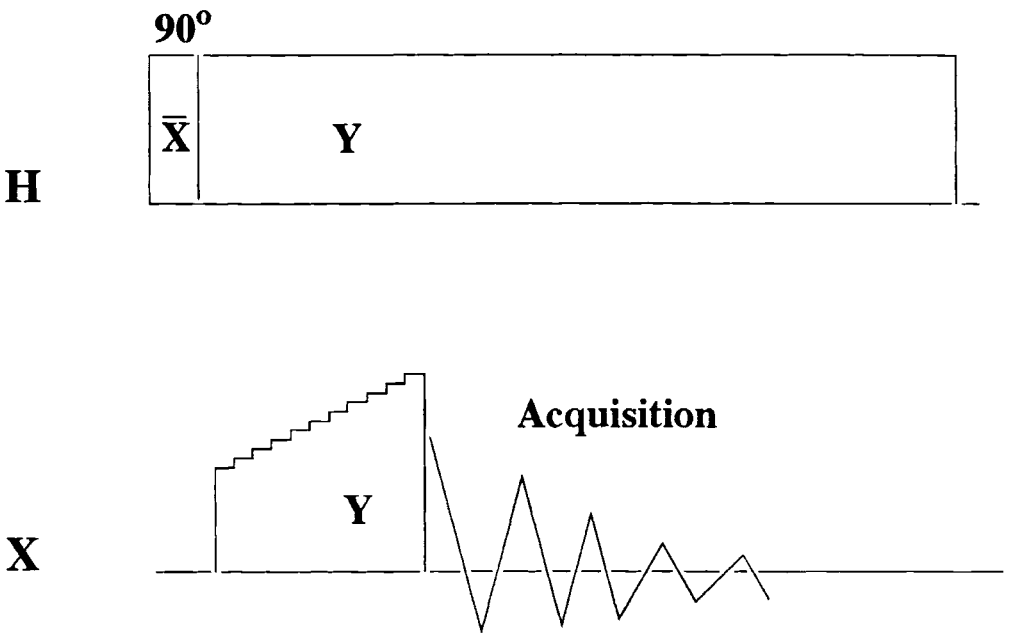

Figure 1. Quasi-adiabatic cross polarization pulse sequence used to obtain the CPMAS spectra with a 90° proton pulse width of 5 μs and cross polarization contact time 2 ms.

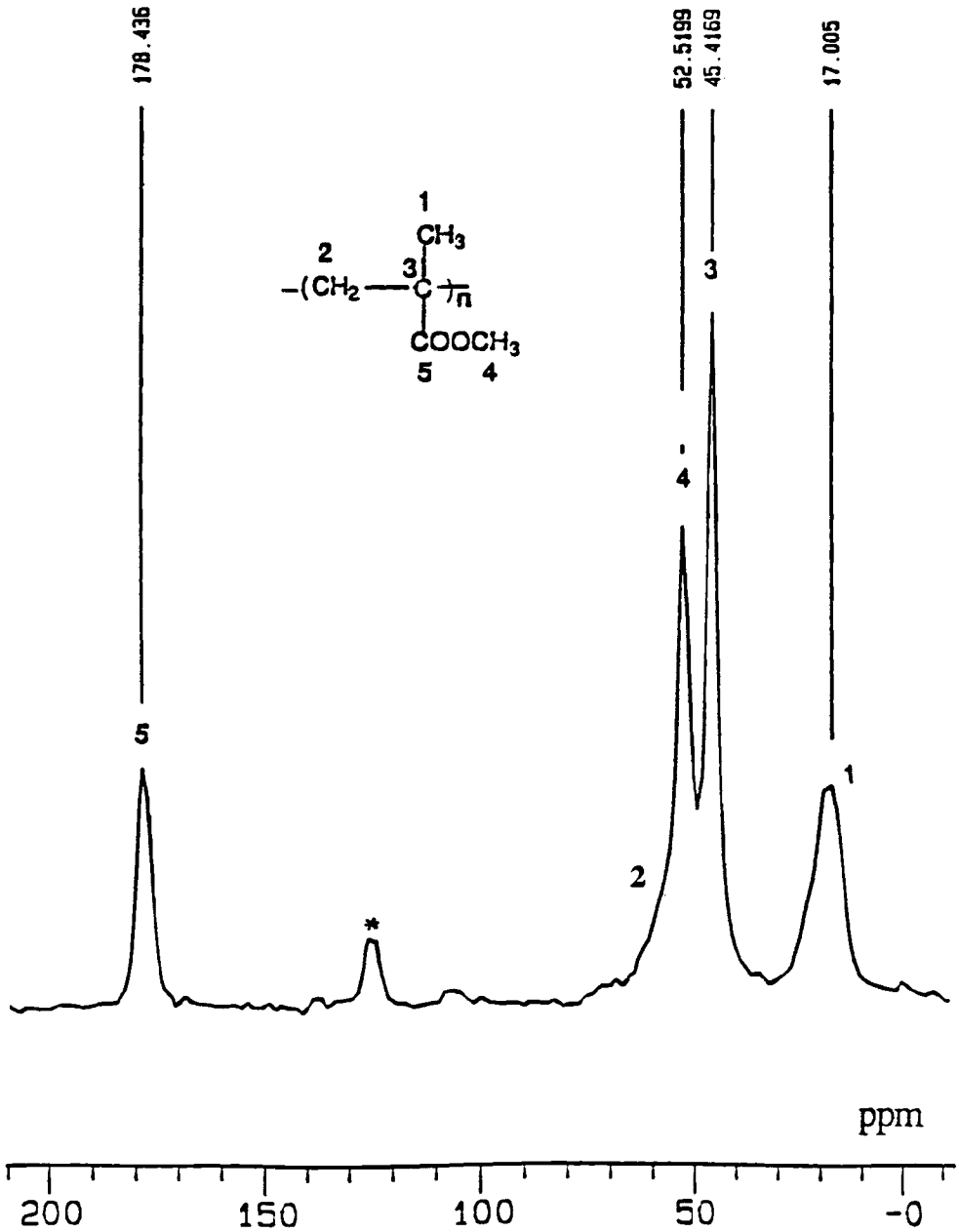

Figure 2. ^{13}C CPMAS spectrum of PMMA. Spinning speed, 4 kHz; 128 scans, 1K data points. Other conditions are in Figure 1. * Represent spinning side band.

shoulder. The carbonyl carbon is at 178 ppm. The peak assignments are in agreement with the earlier reports.[15]

In the colloidal silica sample, incomplete hydrolysis and condensation leaves residual ethoxy groups.[16] The carbon resonances for the ethoxy groups are observed at 18 ppm and 61 ppm in the ^{13}C CPMAS of the sample (Figure 3). TPM modified colloidal silica has seven additional signals as indicated in the spectrum. The spectrum observed (Figure 4) matches well with the earlier report of De Haan and coworkers.[17] They observed 8 resolvable peaks from a sample of commercial silica gel modified with 3-(trimethoxysilyl)propyl methacrylate (TPM). The peak area of the OCH_3 group at 51 ppm, compared to other peaks, suggests that there is approximately one such group per residue of TPM.

Since the bulk of the material in the composite is PMMA, the ^{13}C CPMAS spectrum looks similar to that of the bulk PMMA, obscuring the signals from TPM. However, the small signals observed at 138 ppm and 168 ppm are from the C=C and C=O signals of TPM (Figure 5), respectively. Peak area measurements of the carbonyl at 167 ppm and the carbonyl at 177 pm by simulation of the spectrum reveals that the composite contains about 3% of the unpolymerized TPM. Moreover, the broad shoulder at 66 ppm is from the silane coupling agent.

^{29}Si CPMAS Spectra. The quasi-adiabatic cross polarization pulse sequence was also used to obtain the ^{29}Si CPMAS spectra. The ^{29}Si spectrum of the parent silica (Figure 6) has three signals from Q^2 $\underline{Si}(OCH_2CH_3/OH)_2(OSi)_2$, Q^3 $\underline{Si}(OCH_2CH_3/OH)(OSi)_3$ and Q^4 $\underline{Si}(OSi)_4$ silica regions at -90, -100 and -110 ppm in the spectrum respectively. The peak assignments are in accordance with the earlier reports based on chemical shift correlation and relaxation data reported by Maciel and co-workers.[7]

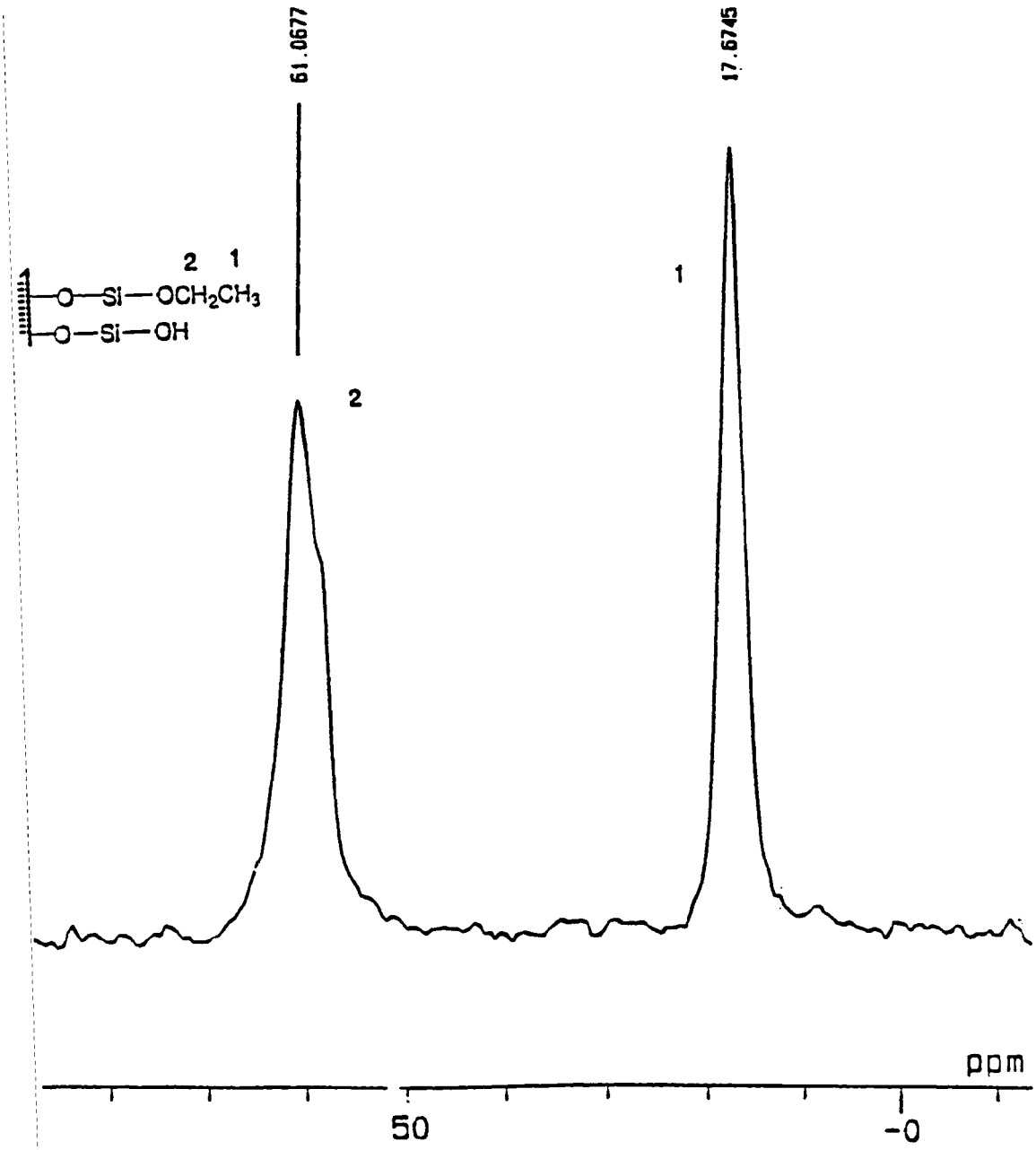

Figure 3. ^{13}C CPMAS spectrum of parent silica, 6400 scans and with similar conditions as in Figure 2.

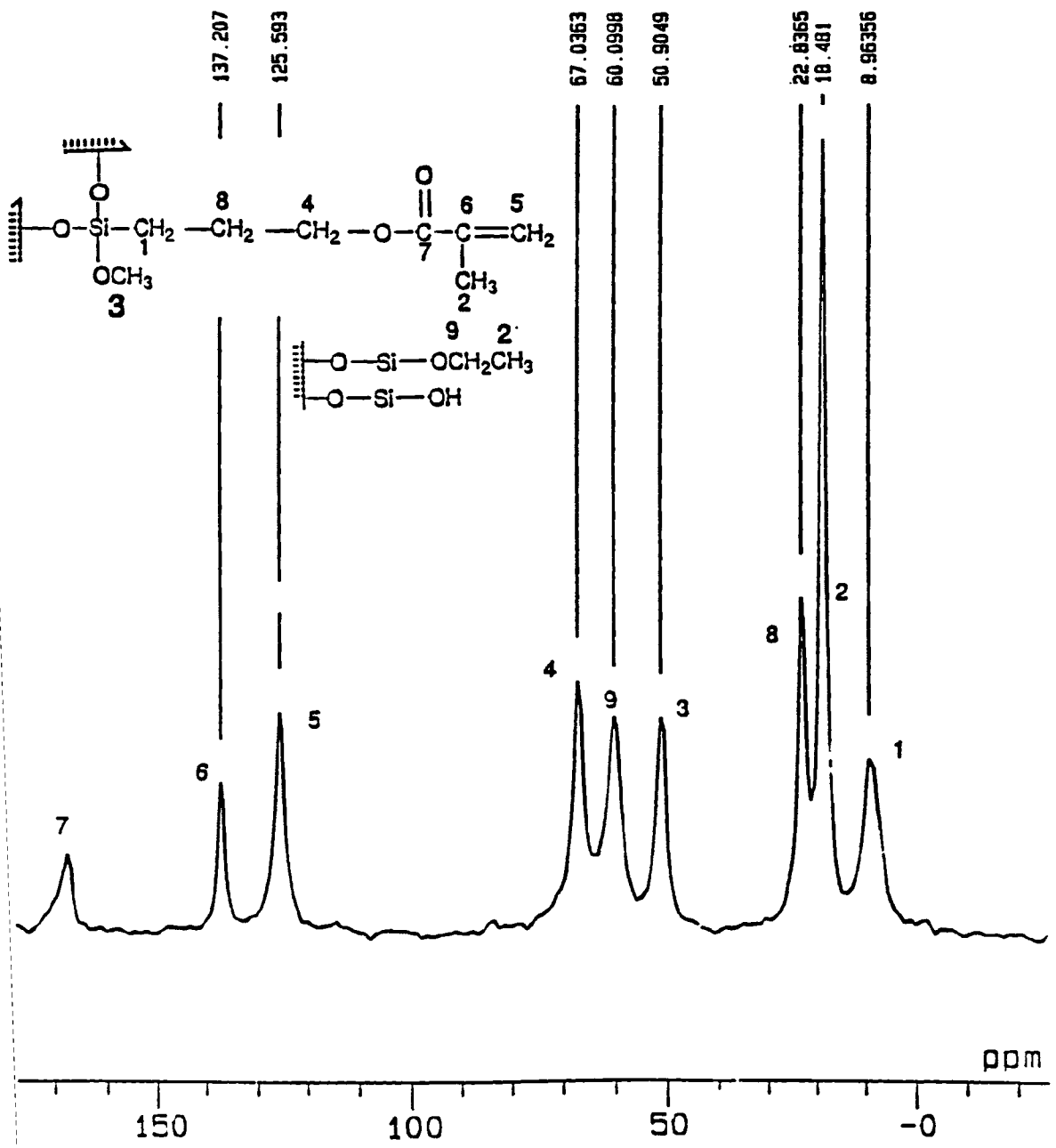

Figure 4. ^{13}C CPMAS spectrum of TPM silica, 2000 scans and with similar conditions as in Figure 2.

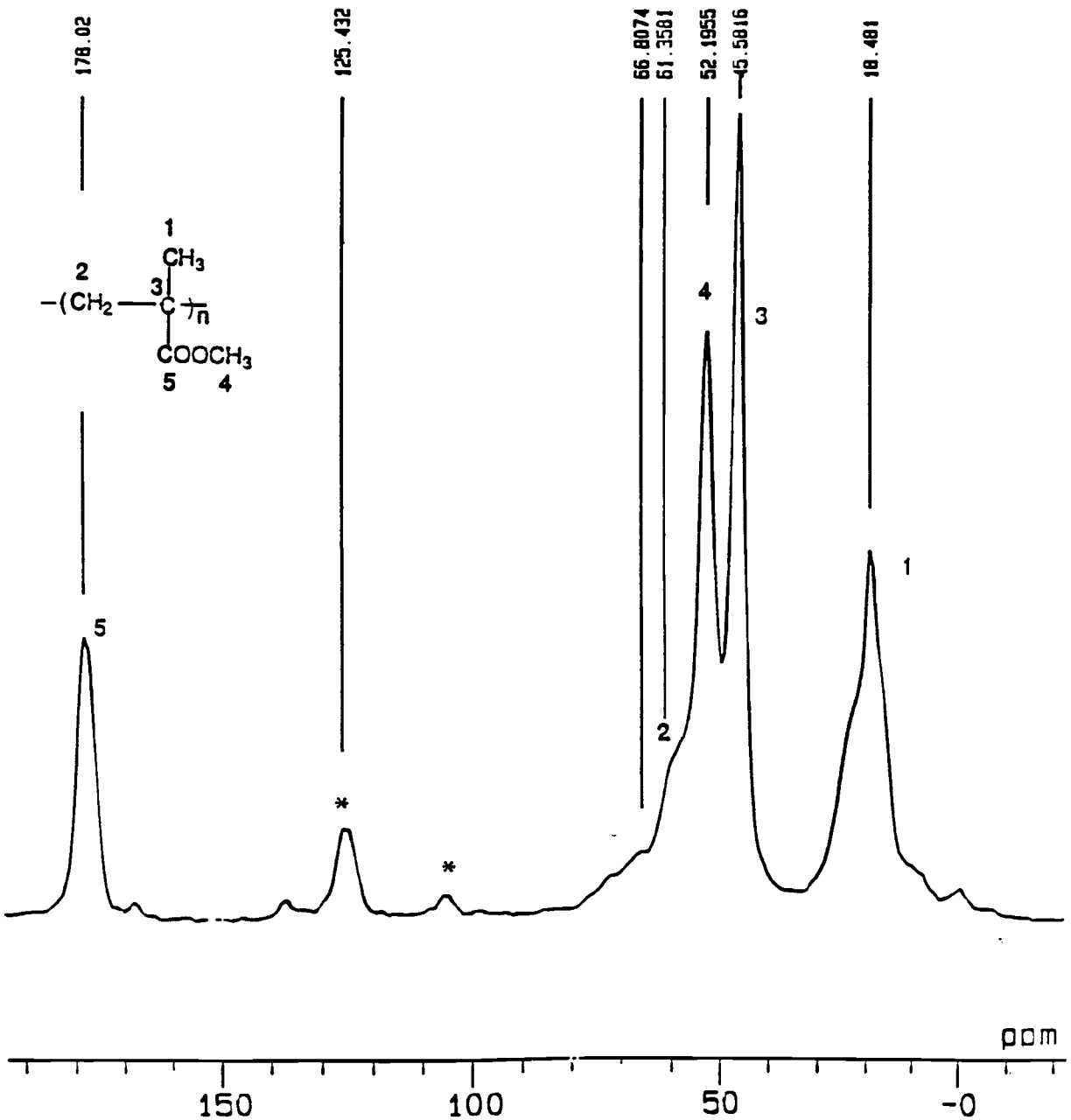

Figure 5. ^{13}C CPMAS spectrum of composite, 2000 scans and with similar conditions as in Figure 2; * represents spinning side bands.

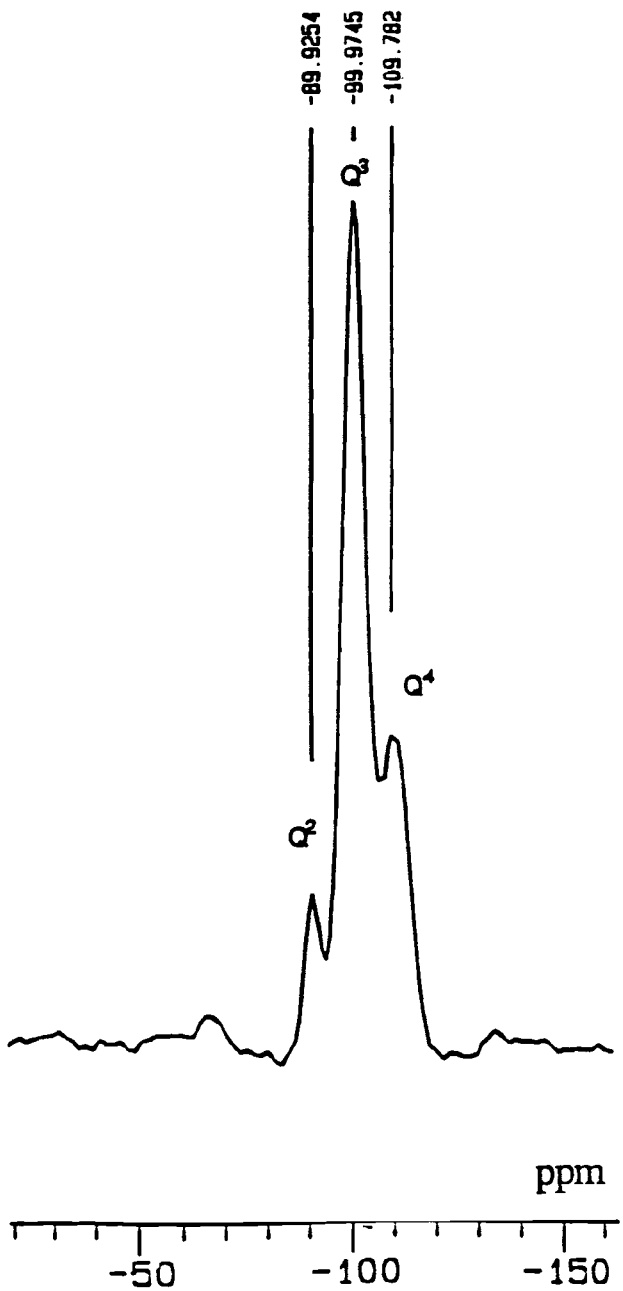

Figure 6. ^{29}Si CPMAS spectrum of parent silica, 512 scans.

Besides the three silicon signals from colloidal silica, TPM-coated silica has a new group of signals at -48 to -65 ppm (Figure 7) from ^{29}Si nuclei designated as S^1 $(SiO)\underline{Si}(OCH_3/OH)_2R'$, S^2 $(SiO)_2\underline{Si}(OCH_3/OH)R'$ and S^3 $(SiO)_3\underline{Si}R'$ where R'= $CH_2CH_2CH_2OC(O)C(CH_3)=CH_2$. The ^{29}Si CPMAS spectrum of the composite also gave six well resolved peaks similar to that of the TPM-modified colloidal silica and is shown in Figure 8.

Deconvoluted ^{29}Si CPMAS spectra were generated using a function consisting of three overlapping gaussian lines. The nine associated variables (width, area and chemical shift for each of the three peaks) were adjusted to obtain a best fit to the experimental spectra. For this the data were transferred to a PC computer (1024 points per spectrum). The results are tabulated in Table I. With cross polarization, not all ^{29}Si atoms are observed, especially the Q^4 environment where the nearest proton is at least four bonds away. The spectra were recorded with a 5 ms contact time with varying numbers of acquisitions to obtain better signal to noise ratio (Figures 6-8).

The peak areas of the Q^4 sites of parent silica (using CPMAS) increase with increasing cross-polarization time, suggesting long cross-polarization time for those sites. The corresponding Q^3 peak areas decrease, and the values are shown in Table II. Thus, the relative peak areas are a balance between the intensity increase with longer cross-polarization time and the corresponding intensity decrease with ^1H spin-lattice relaxation in the rotating frame.

^{29}Si Single Pulse Experiments. ^{29}Si single pulse experiments were performed on the three samples mentioned above. A preliminary study showed that the spin-lattice relaxation times T_1 for the Q^3 and Q^4 resonances in our colloidal silica sample were about 28 and 40 seconds, respectively. This was done by varying the pulse delay time (20 - 800 s) in a direct polarization experiment. The data were fitted to a single exponential function to obtain the spin lattice relaxation time. The result is shown in

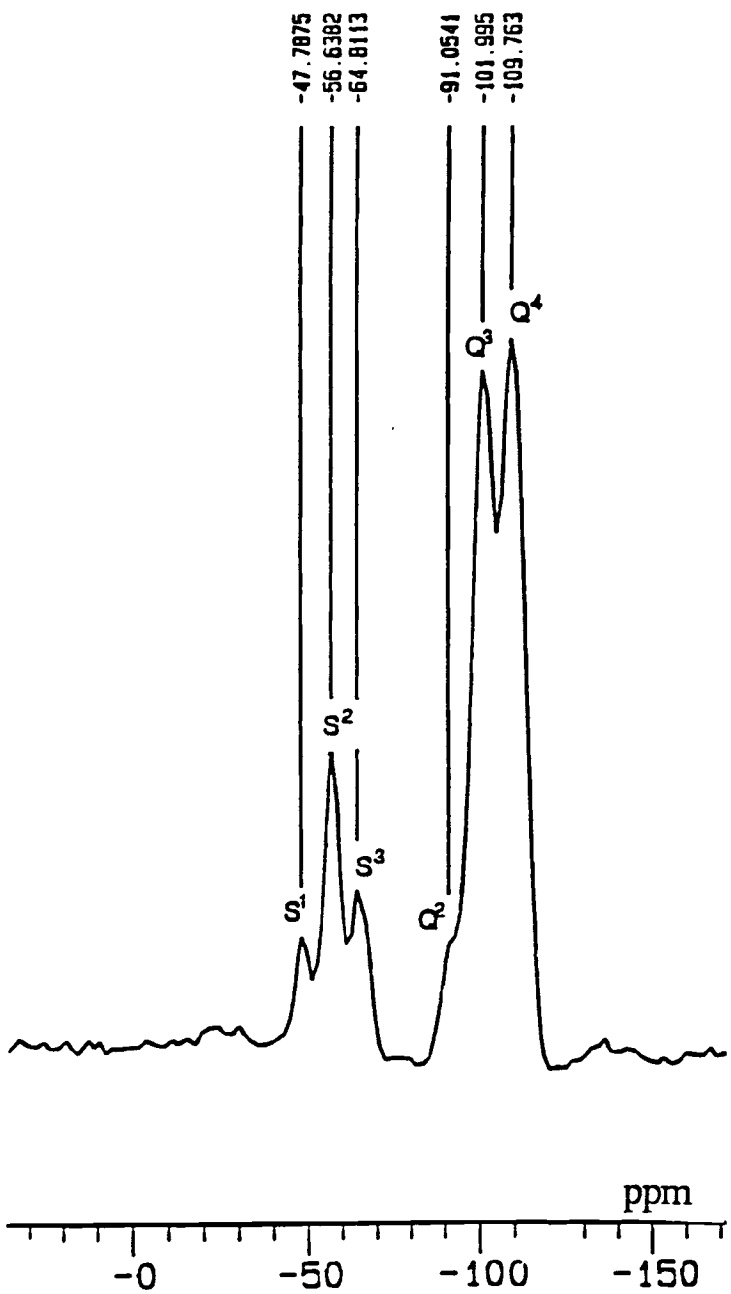

Figure 7. ^{29}Si CPMAS spectrum of TPM silica with similar conditions as in Figure 6.

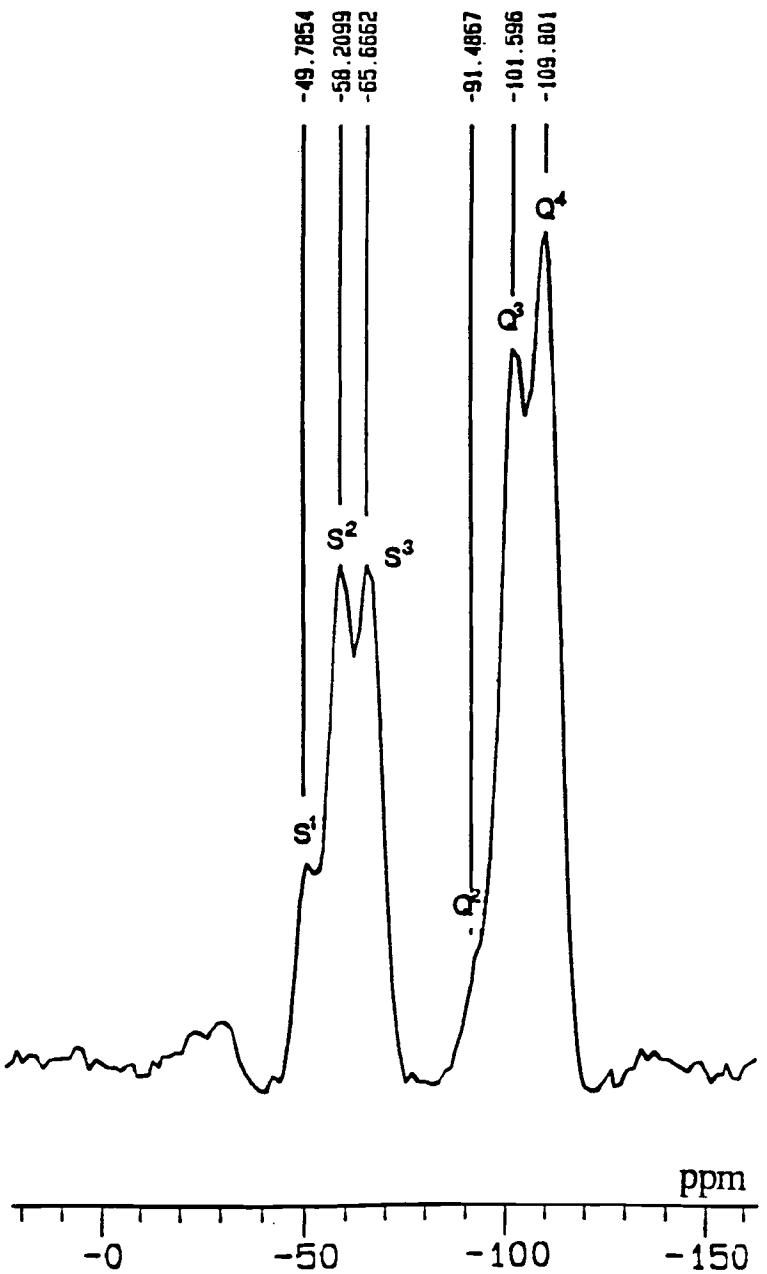

Figure 8. ^{29}Si CPMAS spectrum of the composite, 1800 scans and with similar conditions as in Figure 6.

Table I. Percentage of Si Atoms from ^{29}Si CPMAS Spectra[a]

Sample	Q^2	Q^3	Q^4	S^1	S^2	S^3
Parent Silica	7	66	28			
TPM Silica	6	45	49	20	51	29
Composite	7	41	52	18	41	41

[a]Estimated errors ± 1.

Table II. Percentage of Si Atoms from ^{29}Si CPMAS Spectra of Parent Silica for Various Contact Times[a]

Contact Time (ms)	Q^2	Q^3	Q^4
5	7	66	28
10	7	57	36
15	6	50	44

[a]Estimated errors ± 1.

Figure 9. The Q^4 data do not fit a single exponential well, and some Q^4 Si atoms must have T_1 >> 40 s. The quantitative spectra for the three samples were obtained by choosing a pulse delay time of 200 seconds (5 x T_1) using a spin echo pulse sequence.

Spectra were accumulated from 200 acquisitions. The experimental and the deconvoluted spectra are shown in Figures 10-12. Peak area measurements revealed that about 23% of the total Si sites are from the coupling agent TPM (Figures 11 and 12). Deconvoluting the spectra by assuming gaussian line shapes gave the composition of the corresponding Si atoms (Q and S sites) in these samples. The results are compiled in Table III. Poor S/N in the composite sample does not allow an unambiguous deconvolution for the S sites. The data are derived from the best visual fit.

The percent of Q^4 silicon atoms detected in a CPMAS experiment with a 5 s contact time was calculated as follows. Assume all Q^4 sites are fully relaxed after an 800 s delay in single pulse spectra as shown in Figure 9. The Q^4 signal after a 200 s delay is 93% as great as the signal after 800 s, so the relative areas in single pulse spectra reported in Table III account for 93% of the Q^4 silicon atoms. Normalization of the parent silica results in Table III gives 3% Q^2, 33% Q^3, and 64% Q^4 silicon atoms. Therefore, the unnormalized percentages detected in parent silica by the CPMAS spectrum in Table I are 3% Q^2, 33% Q^3, and 14% Q^4, and the percent of Q^4 atoms detected in the CPMAS spectrum is (14/64) (100) = 22%. The total percent of silicon atoms detected is 3 + 33 + 14 = 50%. The Q^4 silicon atoms not detected in the parent silica sample are not detected in the TPM-silica and composite sample either, and so all CPMAS results refer tyo only the 22% of Q^4 sites detected. Data from Tables I and III also indicate that the Q^4 sites are not affected much on composite formation. The data for Silicon sites (S) in TPM-silica (Table I and II) also shows inefficient cross-polarization, about 78% of the S^3 sites are dected with the contact time of 5 ms.

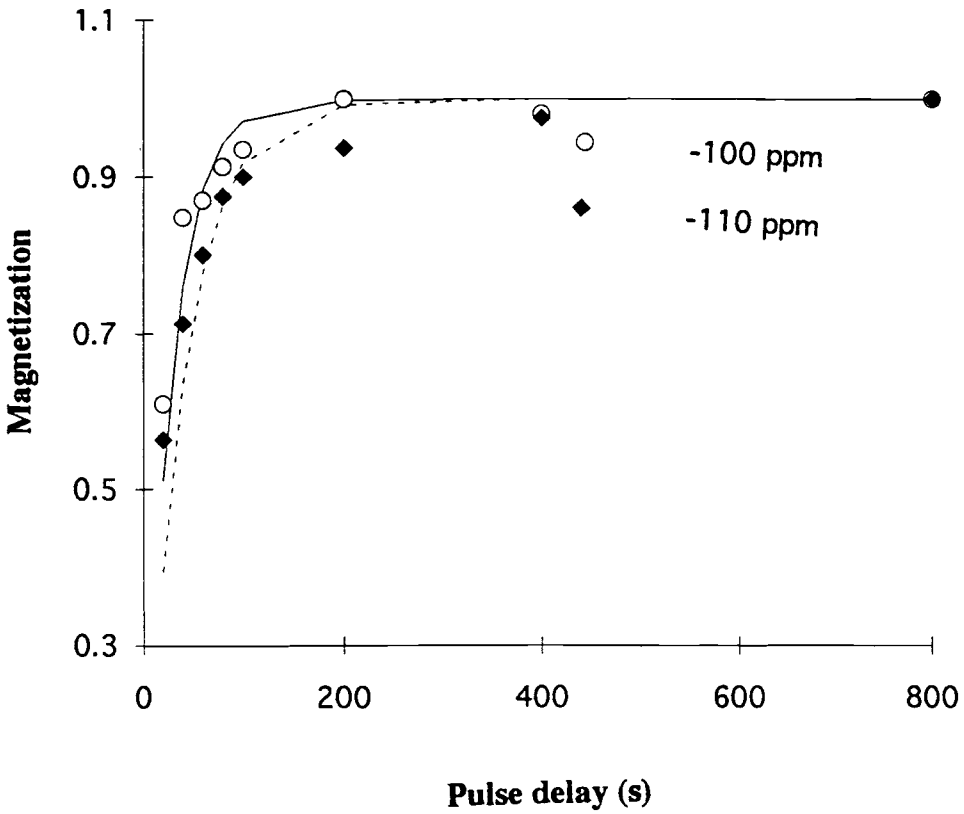

Figure 9. Plot of magnetization recovery for various pulse delay times of Q^3 and Q^4 peaks in parent silica. The solid and the broken lines represent single exponential fit to the experimental values of Q^3 and Q^4 peaks respectively.

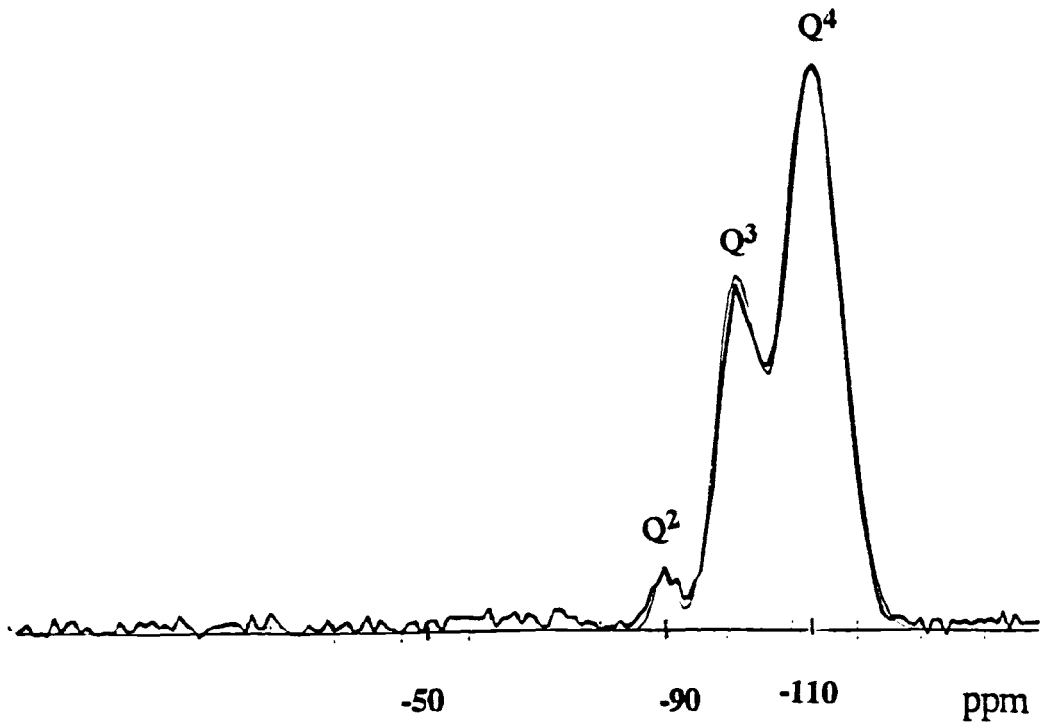

Figure 10. ^{29}Si single pulse spectrum of parent silica. The thin line is the simulated spectrum and the thick line is the experimental spectrum.

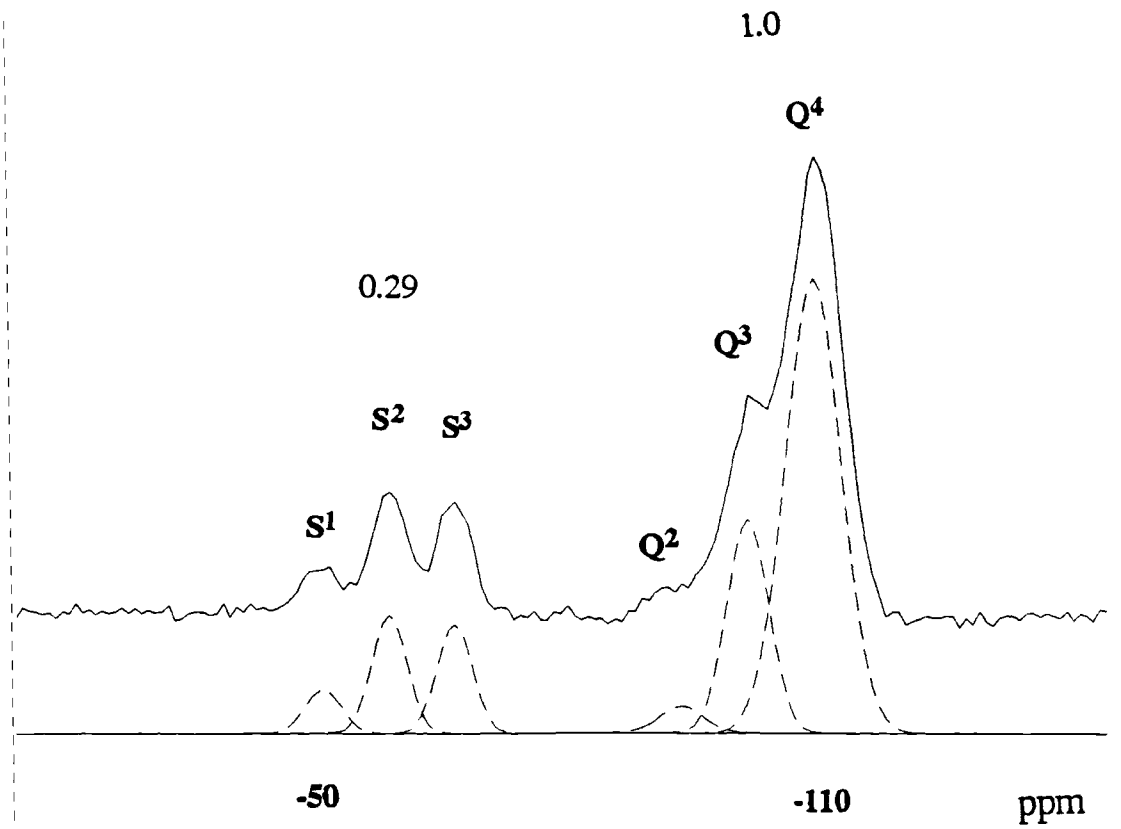

Figure 11. ^{29}Si single pulse spectrum of TPM silica. The dashed line is the simulated spectrum and the thick line is the experimental spectrum. Figures on top of the peaks represents peak areas obtained by electronic integration.

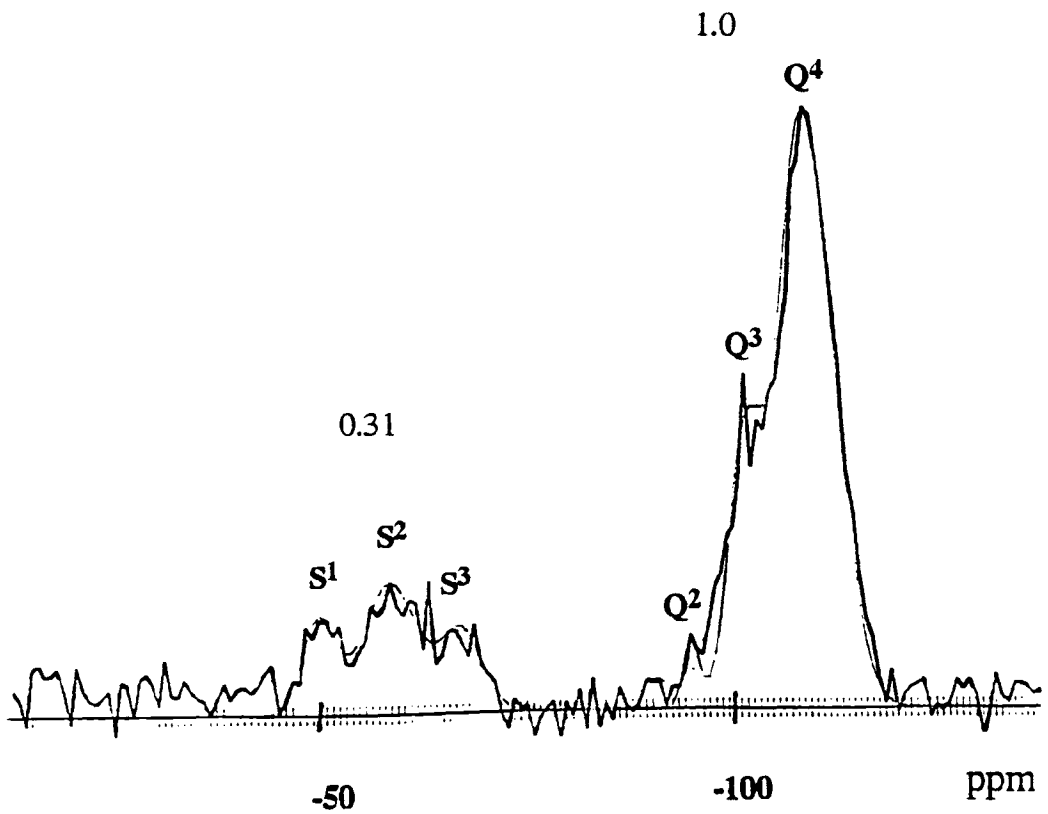

Figure 12. ^{29}Si single pulse spectrum of the composite. The thin line is the simulated spectrum and the thick line is the experimental spectrum. Figures on top of the peaks represents peak areas obtained by electronic integration.

Table III. Percentage of Si Atoms from ^{29}Si Single Pulse Spectra

Sample	Q^2	Q^3	Q^4	S^1	S^2	S^3
Parent Silica[a]	3	35	62			
TPM Silica[a]	3	25	72	17	43	40
Composite[a]	3	21	76	22[b]	37[b]	41[b]

[a]Estimated errors ± 1. [b]Estimated error ± 3.

Some of the Q^3 sites in the parent silica are converted into Q^4 sites when the surface is modified with TPM. The decreased intensity of the isolated silanol absorption peak at 3743 cm^{-1} in the DRIFT spectrum (Figure 13) supplements the above observation. The broad absorption band in parent silica from 3700 cm^{-1} to 3000 cm^{-1} can be attributed to hydrogen-bonded silanols (3660 cm^{-1}) and absorbed water (3520 and 3400 cm^{-1}) based on earlier studies.[18] The sharp peak at 3743 cm^{-1} has been assigned to the freely vibrating surface hydroxyl groups, the isolated silanols. In the DRIFT spectrum of the TPM silica, the O-H stretching region becomes narrower because the TPM reacts with the hydrogen bonded silanols and the isolated silanols. The peak at 1625 cm^{-1} is due to molecular water on the surface and is absent in the composite spectrum (Figure 13).

T_{1H} Measurements. T_{1H} was measured via detection of ^{13}C and ^{29}Si. Proton T_1 values were measured by a pulse sequence involving saturation and recovery of the proton magnetization, followed by cross-polarization to ^{13}C or ^{29}Si to observe the resultant magnetization. The conventional saturation recovery pulse program was modified to include the quasi-adiabatic cross-polarization sequence for the detection of the resultant magnetization. The pulse sequence is shown in Figure 14. A saturation pulse of 1 ms duration was employed to null the proton magnetization. The mechanical properties of composite materials are related to motions of the polymer molecules. Spin-lattice relaxation rates (R_1) controlled by the dipolar mechanism are sensitive to motions which occur at a rate comparable to the NMR frequency. The general rate expressions for dipolar relaxation in the laboratory frame are given by the equations

$$(R_1) = 2\gamma^4 h^2 I(I+1)\,[\tau_c/(1+\omega^2\tau_c^2) + 4\tau_c/(1+4\omega^2\tau_c^2)]/5r^6 \qquad (2)$$

$$(R_2) = \gamma^4 h^2 I(I+1)\,[3\tau_c + 5\tau_c/(1+\omega^2\tau_c^2) + 2\tau_c/(1+4\omega^2\tau_c^2)]/5r^6 \qquad (3)$$

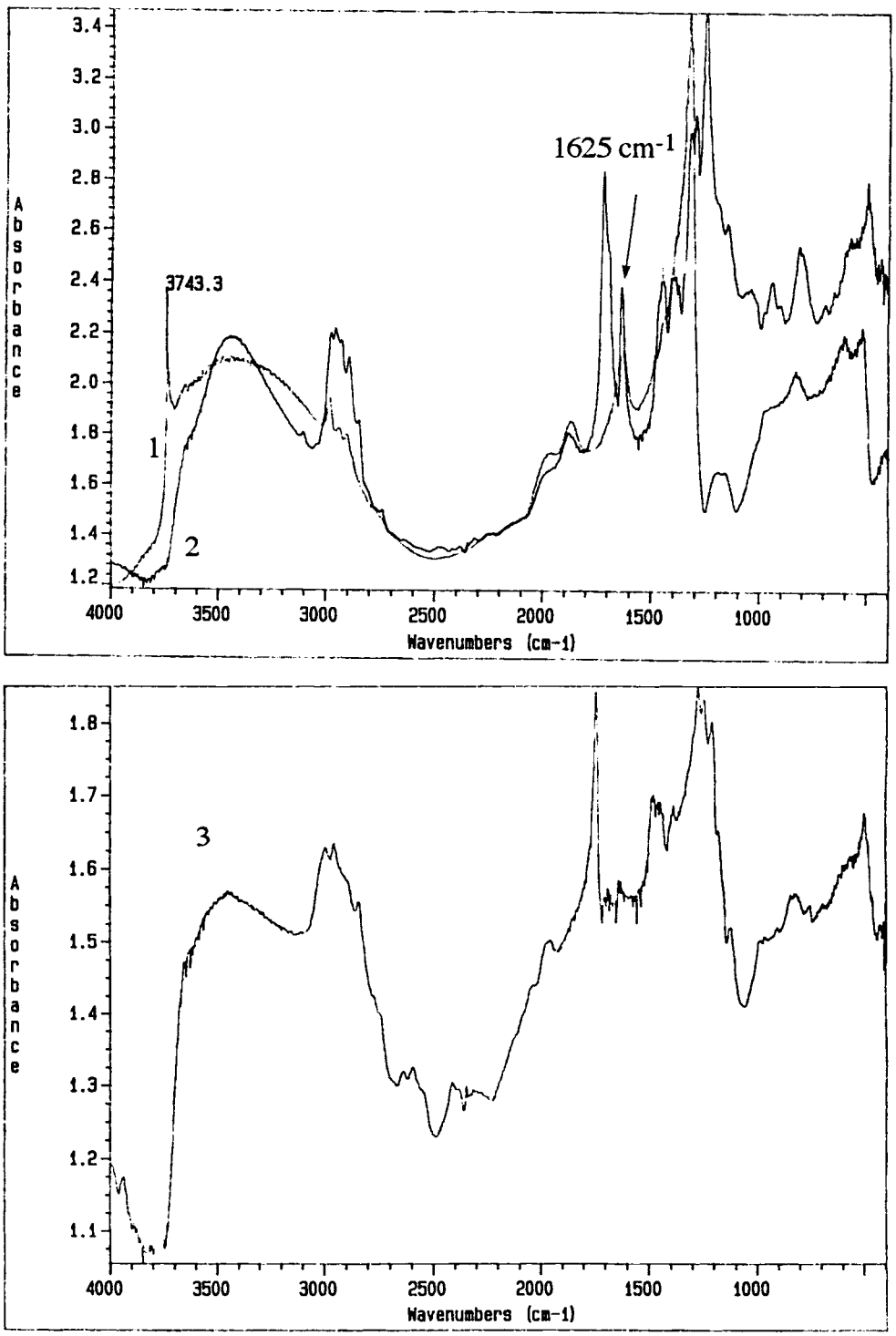

Figure 13. DRIFT spectra of parent silica (1), TPM silica (2), and composite (3).

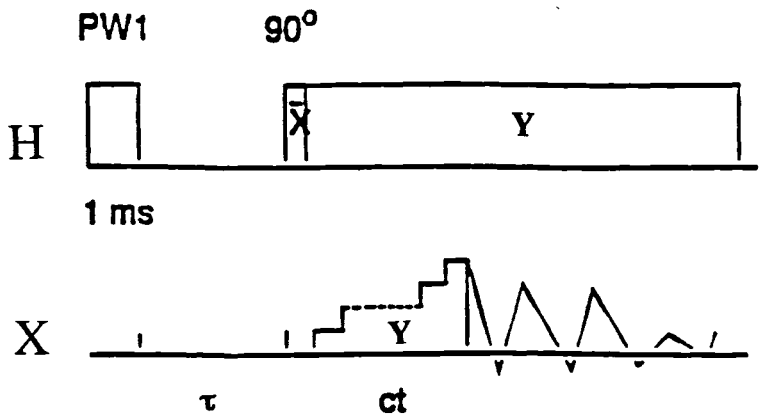

Figure 14. T_{1H} pulse sequence; ct is the cross polarization contact time and PW1 is the saturation pulse.

where R_1 is spin-lattice relaxation rate, R_2 is spin-spin relaxation rate, γ is the magnetogyric ratio, h is Planck's constant, I is the spin quantum number, ω resonance frequency, and τ_c molecular rotational correlation time.[19] The expression for R_1 predicts a minimum in a plot of $1/R_1$ versus 1/T near $\omega\tau_c \sim 1$ and is sensitive to motions in this region, where $\tau_c \sim 1/\omega$.

The spin lattice relaxation behavior can be described as an exponential function.[20]

$$M_{(\tau)}/M_o = 1-\exp(-\tau/T_1) \qquad (4)$$

The time constant T_1 was calculated by a single exponential fit to the experimental data (Figure 15) as the magnetization is given by the above equation. The T_{1H} values thus obtained are shown in Table IV.

With each sample, the T_{1H} values were similar for all the signals through ^{13}C and ^{29}Si detection. This suggests that the protons from the different environments, like OCH_2CH_3, geminal silanol, isolated silanols, and hydrogen bonded silanols, are strongly dipolar coupled and interact extensively with each other so that they all relax together. A stack plot of the T_1 measurement for parent silica is presented in Figure 16. One can see the evolution of the three Si resonances as a function of various delay times. Moreover the T_1 values are the same in all three samples. The ^{13}C and ^{29}Si peaks in all samples have T_{1H} in the range from 0.5 to 0.6 seconds. Therefore, spin diffusion equilibrates magnetization at all sites in much less than 0.5 seconds.

$T_{1\rho H}$ Measurements. The spin lattice relaxation in the rotating frame is effected by kHz frequency motions, whereas spin lattice relaxation is effected by MHz frequency motions. $T_{1\rho}$ values are difficult to interpret since the relaxation time is sensitive to both spin-lattice and spin-spin relaxation processes. Longer T_{1H} than $T_{1\rho H}$ shows less motion at MHz than at kHz frequencies.

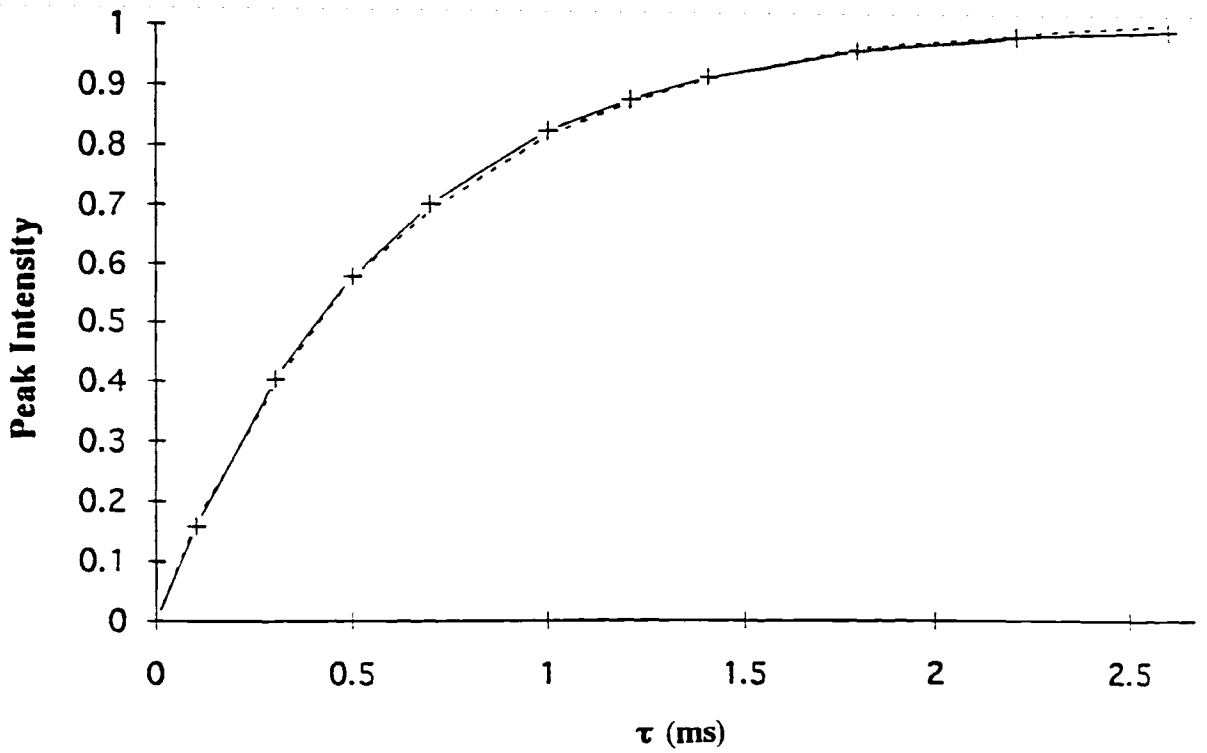

Figure 15. Magnetization recovery of the parent silica Q^3 peak (-100 ppm) in T_{1H} pulse sequence. The + marks represent experimental data, and the broken line is the single exponential simulation.

Table IV. T_{1H} Values in Seconds through ^{13}C and ^{29}Si Detection

Peaks	Parent Silica	TPM Silica	Composite	PMMA
		^{13}C Data[a]		
-C=O (PMMA)			0.58	0.58
-C=O (TPM)		0.58		
-C=		0.55		
$=CH_2$		0.50		
$-OCH_2$		0.50		
$-OCH_2CH_3$	0.60	0.52		
$-OCH_3$		0.55	0.57	0.56
-C-			0.55	0.58
$-Si-CH_2CH_2$		0.50		
$-C-CH_3$	0.50	0.55	0.57	0.60
$-Si-CH_2$		0.45		
		^{29}Si Data[a]		
Q^4	0.55	0.53	0.47	
Q^3	0.58	0.52	0.50	
Q^2	0.70	0.50	-	
S^3		0.50	0.50	
S^2		0.50	0.55	
S^1		0.52	-	

[a] Estimated error limits ± 10%.

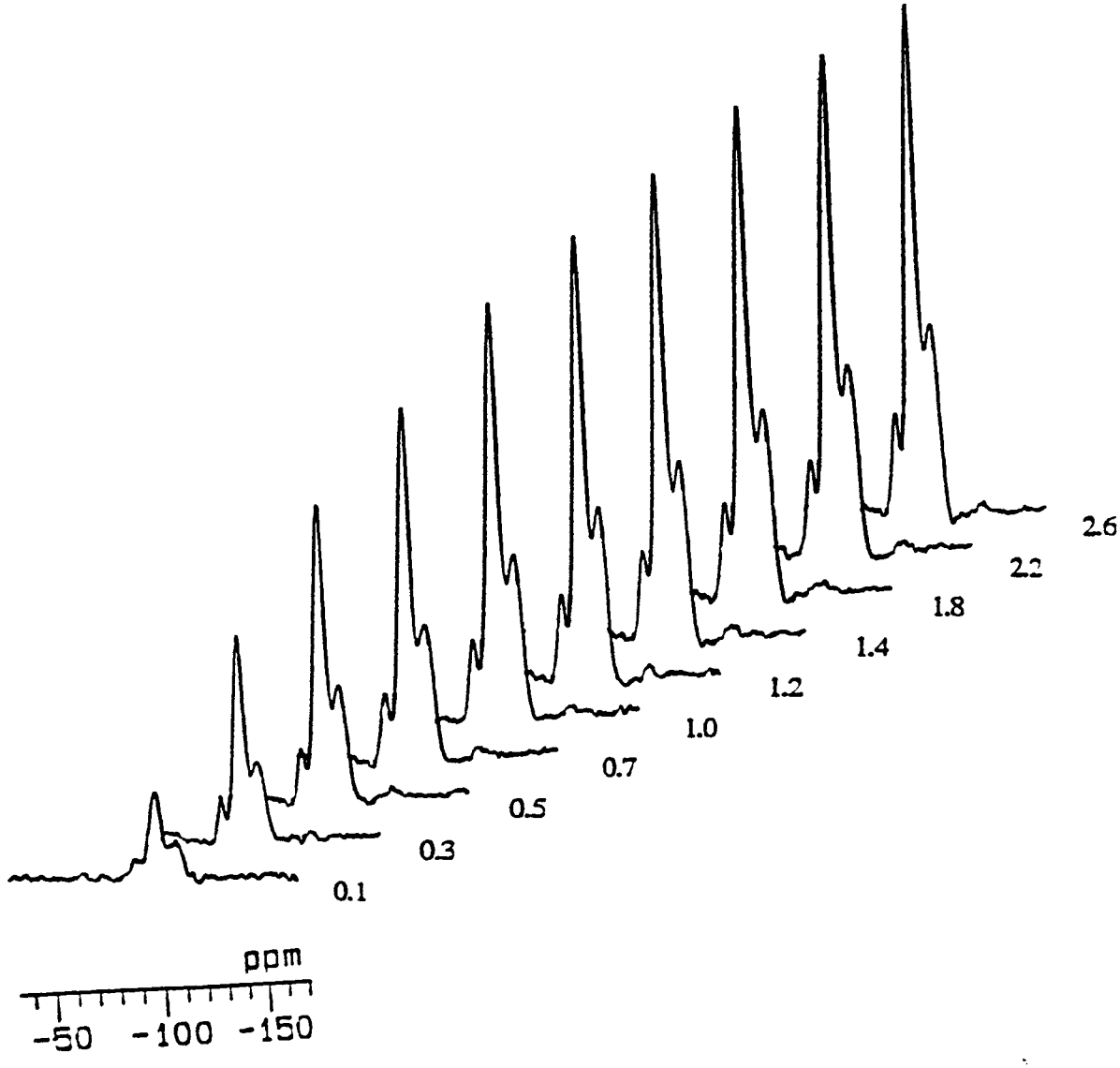

Figure 16. Stack plot of ^{29}Si parent silica T_{1H} relaxation measurements; 256 scans. The delay time τ is in seconds.

In the rotating frame, the relaxation rate $R_{1\rho}$ is more sensitive to molecular mobility. Since the range of applied field is in kHz, it can map molecular motions in this range. In solids the local magnetic field at a nucleus has a strong contribution from static magnetic dipolar fields B_{loc} that originate with neighboring nuclei. Thus B_{loc} is the dominating effective field in the rotating frame. This leads to the expression[19]

$$R_{1\rho} \propto B_{loc}^2 \tau_c/(1 + 4\omega_1^2\tau_c^2) \quad (5)$$

where ω_1 is the precession frequency of the nuclei in the applied field H_1, and hence, $R_{1\rho}$ depends on the applied field.

$T_{1\rho H}$ was measured via detection of ^{13}C and ^{29}Si. The pulse sequence used is shown in Figure 17. After a 5 μs 90° ^1H pulse for ^{13}C detection, or 6 μs for ^{29}Si detection, the proton magnetization is spin locked for a variable period τ. The spin lock fields $(\gamma_H/2\pi)B_{1H}$ were 50 kHz and 42 kHz for ^{13}C and ^{29}Si, respectively. The residual signal was detected through the QACP sequence.

The motional behavior of distinct environments of the silane coupling agent in the kHz range can be described by the spin-lattice relaxation parameters in the rotating frame. A graphical method for determining the decay time constant is given by the following equation,[20]

$$\ln (Y_i - Y_o) = -\tau/T_1 + \text{constant} \quad (6)$$

where Y_o is the initial magnetization taken at the first τ value and Y_i is the magnetization at successive τ values for i^{th} time. Time constant T can be obtained form the slope of plot of $Y_i - Y_o$ versus τ for a given set of data . Since it is difficult to estimate M_o, the thermal equilibrium magnetization in equation 4, the exponential decay equation can be modified further as

$$M_{(\tau)} = A \exp(-\tau/T_1) + B \quad (7)$$

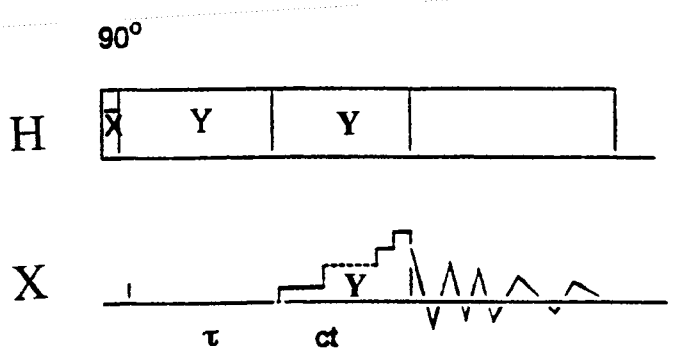

Figure 17. $T_{1\rho H}$ pulse sequence.

Table V. $T_{1\rho H}$ Values in Milliseconds through ^{13}C and ^{29}Si Detection

Peaks	Parent Silica	TPM Silica	Composite	PMMA
		^{13}C Data[a]		
-C=O (PMMA)			13	12
-C=O (TPM)		6.3		
-C=		5.5		
$=CH_2$		4.4		
$-OCH_2$		4.7		
$-OCH_2CH_3$	52	5.6		
$-OCH_3$		5.8	13	14
-C-			13	14
$-Si-CH_2CH_2$		5.6		
$-C-CH_3$	42	5.5	12	14
$-Si-CH_2$		5.6		
		^{29}Si Data[a]		
Q^4	31	4.8	9	
Q^3	29	4.8	9	
Q^2	26	5.0	-	
S^3		4.0	11	
S^2		5.0	11	
S^1		-	12	

[a] Estimated error limits ± 10%.

where $M_{(\tau)}$ represents the fraction of magnetization left to recover, A contains information about initial magnetization and, B about the thermal equilibrium magnetization. $T_{1\rho H}$ values were calculated from equation 6 or by an exponential fit (equation 7) and are tabulated in Table V. A representative plot is shown in Figure 18.

Many studies have shown that the presence of flexible chains on the silica surface quenched the spin diffusion and strongly reduced dipolar interactions.[21,22] Longer $T_{1\rho H}$ for the parent silica suggests that there is motional freedom with the ethoxy and hydroxy groups in the sample, and less efficient relaxation. The longer $T_{1\rho H}$ values detected by ^{13}C than by ^{29}Si for parent silica means that spin diffusion between C-H and O-H groups is not completely efficient, and that the O-H groups have more kHz frequency motions than the OCH_2CH_3 groups. $T_{1\rho H}$ values from 26-31 ms for ^{29}Si detection and 42-52 ms for ^{13}C detection indicates spin diffusion between C-H and O-H protons is incomplete in 50 ms.

When the silane coupling agent is anchored onto the silica, there is about an eight fold decrease in $T_{1\rho H}$ through ^{13}C detection and about 6 fold decrease through ^{29}Si detection, and all signals show the same $T_{1\rho H}$ as reported in Table V. This suggests that the spin diffusion process is efficient in the TPM layer. The same $T_{1\rho H}$ throughout the composite shows that there is intimate mixing between PMMA and polymerized TPM silica in the composite sample. This also suggests that the attachment of the silane coupling agent through the condensation reaction replaces many ethoxy groups from the surface besides the silanol protons. Much shorter $T_{1\rho H}$ than in parent silica shows more proton motion at 50 kHz in the TPM layer. Since all values are in the range of 4-6 ms, there is rapid spin diffusion among all ^1H sites in $<< 5$ ms, even those that cross polarize with ^{29}Si.

In composite, the $T_{1\rho H}$ values are due mainly to the large pool of protons from the bulk PMMA matrix. The presence of TPM silica in the PMMA matrix has little effect, as

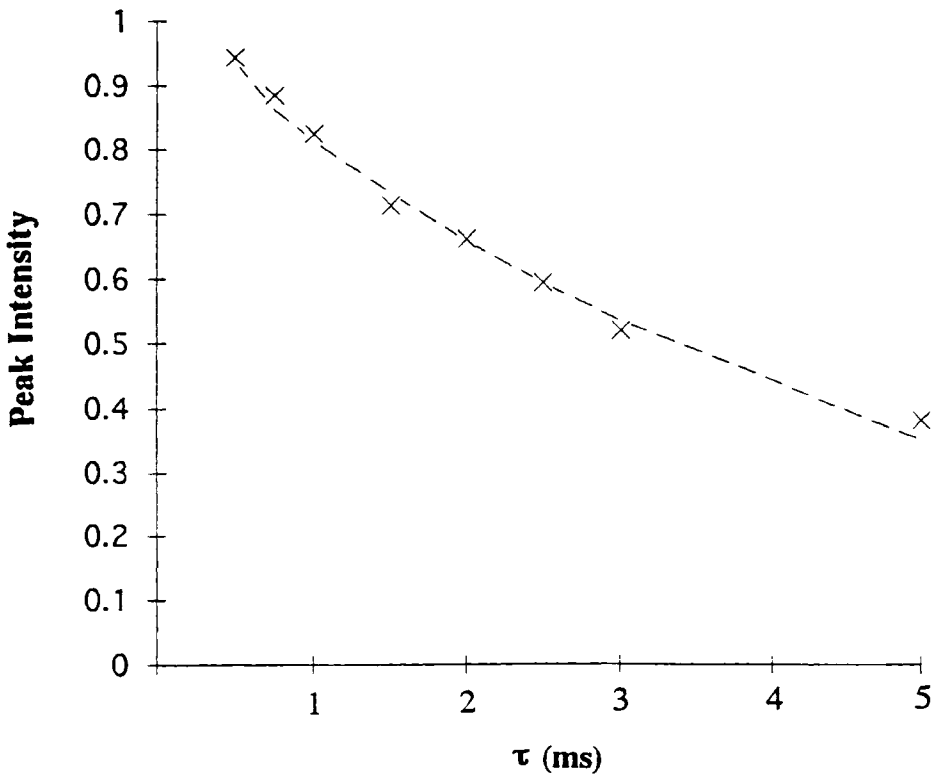

Figure 18. Magnetization decay of the TPM silica Q^3 peak (-100 ppm) in $T_{1\rho H}$ pulse sequence. x represents experimental data, and the broken line is the single exponential simulation.

the $T_{1\rho H}$ values are similar for the composite and PMMA. A stack plot of ^{29}Si TPM silica $T_{1\rho H}$ relaxation measurement is shown in Figure 19. $T_{1\rho H}$ values about 11-14 ms at all but Q^4 and Q^3 sites prove intimate mixing of TPM and PMMA with rapid spin diffusion in << 11 ms. Slightly shorter $T_{1\rho H}$ values at Q^3 and Q^4 sites suggest that some of them do not equilibrate so rapidly by spin diffusion and are more isolated.

$T_{1\rho C}$ Measurements. A direct interpretation of the $T_{1\rho H}$ measurements to describe the molecular motions is not possible, as $T_{1\rho H}$ is an average of all the protons in the sample due to spin diffusion. This is not a problem with the carbon $T_{1\rho C}$ experiment. Because ^{13}C has low natural abundance, the physical separation between ^{13}C atoms is large, and the spin diffusion rate is low. The pulse sequence is shown in Figure 20. After a 90° pulse, the proton magnetization is cross polarized to carbon, and then the carbon channel is spin locked at 50 kHz for a variable delay period during which the signal decays. The residual magnetization is then detected while decoupling the proton channel. $T_{1\rho C}$ depends on motions at spin lock (50 kHz) frequencies.

The $T_{1\rho C}$ values determined by equation 6 or 7 from experimental data are given in Table VI. During the evolution period τ in the pulse sequence (Figure 20) there is no RF field in the proton channel. The proton magnetization then decreases towards thermal equilibrium with a relaxation time depending on the speed of the rotor. For rapid spinning, this relaxation time is short, and the proton magnetization decreases rapidly. There is magnetization transfer between ^{13}C spins that have low spin temperature and the proton nuclei that have lost their magnetization. Hence, in the measurement of the $T_{1\rho C}$ there is a small contribution from the spin-spin cross polarization time between ^{13}C and proton spins in the equation 5.[23] According to the equation the relaxation rate depends on static magnetic dipolar fields B_{loc} from the neighbouring protons, the precession frequency ω_1 in the spin-lock field, and the rotational correlation time τ_c. The molecular motion depends on B_{loc} and τ_c when the protons are directly bound to the carbon.

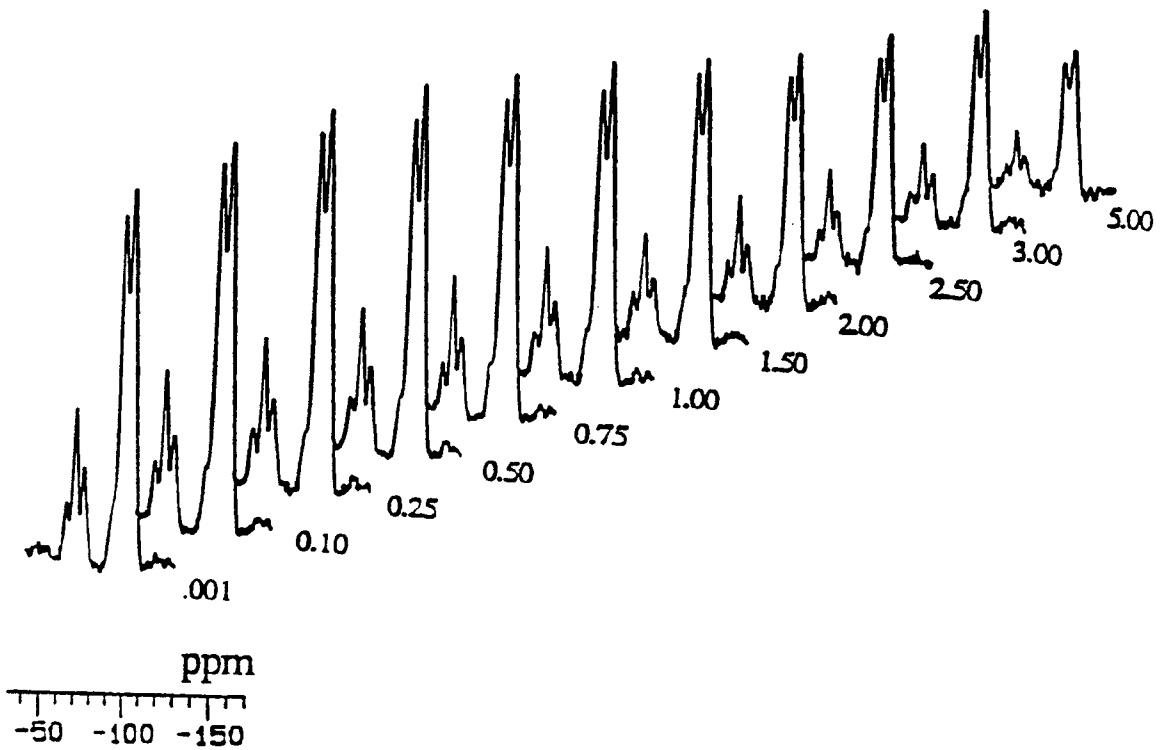

Figure 19. Stack plot of ^{29}Si TPM silica $T_{1\rho H}$ relaxation measurements; 256 scans. The delay time τ is in milliseconds.

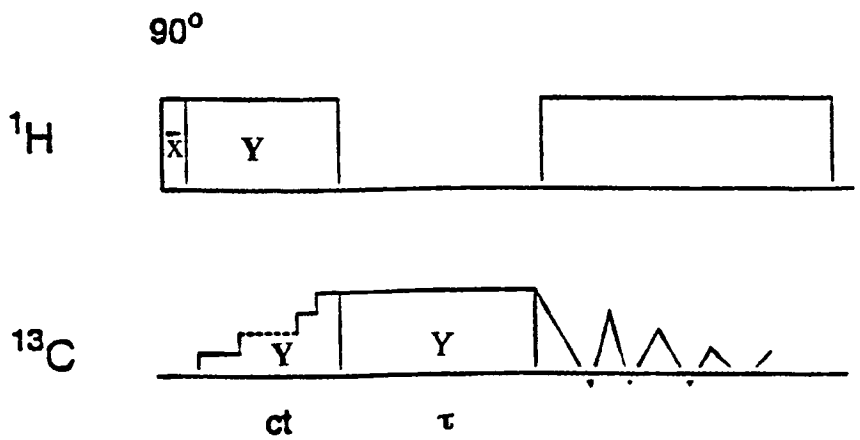

Figure 20. $T_{1\rho C}$ pulse sequence.

Table VI. $T_{1\rho C}$ Values in Milliseconds[a]

Peaks	Parent Silica	TPM Silica	Composite	PMMA
-<u>C</u>=O (PMMA)			103	105
-<u>C</u>=O (TPM)		55		
-<u>C</u>=		30		
=<u>C</u>H_2		8		
-O<u>C</u>H_2		7		
-O<u>C</u>H_2CH_3	65	12		
-O<u>C</u>H_3		27	50	65
-<u>C</u>-			130	140
-Si-CH_2<u>C</u>H_2		7.		
-C-<u>C</u>H_3	80	42	25	20
-Si-<u>C</u>H_2		7		

[a] Estimated error limits ± 10%.
All values obtained from the initial part (maximum $\tau = 2$ ms) of the decay curve.

Long $T_{1\rho C}$ values in parent silica indicate inefficient relaxation with most motions at either >> 50 kHz or << 50 kHz. Lower values of $T_{1\rho C}$ in the TPM modified silica than in the parent silica reveal that the motion of TPM bound to the silica surface is more effective at dipolar relaxation. The TPM silica $T_{1\rho C}$ values of 6.5-8 ms for all protonated C atoms of the TPM group indicate many bond rotations at about 50 kHz. Longer $T_{1\rho C}$ (~42 ms for C-$\underline{C}H_3$ and $CH_2\underline{C}H_3$, and 27 ms for OCH_3) indicates rotation about C-C and O-C has fewer 50 kHz frequencies. The carbonyl and >C= carbons have longer $T_{1\rho C}$ values of 55 ms and 30 ms, respectively, due to longer distance between ^{13}C and ^{1}H nuclei.

$T_{1\rho C}$ of 12 ms for $O\underline{C}H_2CH_3$ in TPM silica compared with 65 ms in parent silica suggests that the rapid motions in the latter are slowed down when the parent silica reacts with TPM, or those rapidly moving $O\underline{C}H_2CH_3$ groups are replaced with TPM during the reaction. Long values of $T_{1\rho C}$ in composites and near identity to those of PMMA itself indicate that PMMA has fewer motions at 50 kHz than does the TPM layer (Table VI). The shorter $T_{1\rho C}$ for C-$\underline{C}H_3$, which has greater mobility than OCH_3 group,[22,23] indicates that most PMMA motions are at < 50 kHz. Similar values for PMMA and composite suggests that the presence of TPM silica in the composite does not affect the mobility of the PMMA matrix.

Spin-lattice relaxation (laboratory frame) of PMMA in the solid state has been studied earlier, and the relaxation data obtained for different carbon environments in those studies did not agree with each other. Schaefer and co-workers[24] reported that the quaternary carbon had a faster relaxation rate than the other carbons. This seems to be unlikely since there are no protons associated to be strongly dipolar coupled. They also found that the α-methyl group had the longest $T_{1\rho}$ value which was associated with its motional freedom.

In another study, Veeman and Edzes[25] found that the relaxation of methoxy and quaternary carbons were non-exponential over a 16 second delay period, and the relaxation rate of the quaternary carbon was slower by a factor of 60 than that of the α-methyl carbon. Methylene and carbonyl carbons had relaxation rate similar to that of the quaternary carbon. Our results for the PMMA (Table VI) are in agreement with the results of Veeman and Edzes.[25] There is a fast relaxing component and a slow relaxing component associated with the α-methyl group. This has been attributed to different tacticities. In the composite, the relaxation data for each of the carbon resonances do not fit a single exponential. There are an initial fast and then a slow relaxation component as shown in Figure 21.

^{1}H -^{1}H Dipolar Dephasing (SDDH). Figure 22 shows the pulse sequence of ^{1}H-^{1}H dipolar-dephasing experiment. After an initial 90^o pulse on ^{1}H channel and prior to cross polarization, there is a ^{1}H-^{1}H dipolar-dephasing period with decoupling in the X channel. During this time changes in proton spin states and homonuclear dipolar interactions cause a non refocusable decay of transverse magnetization. Strongly coupled protons decay at a faster rate, and the residual magnetization is allowed to equilibrate and is detected by the QACP sequence. The dipolar-dephasing time constants (T_{dH}) were calculated from equation 6 and are given in Table VII. A representative plot is as shown in Figure 23.

In ^{13}C detection the T_{dH} values for various peaks within one sample are similar but differ considerably among the samples. In parent silica all the protons detected through ^{13}C have short ^{1}H-^{1}H distances that lead to stronger dipolar interactions. Some protons detected by ^{29}Si have longer T_{dH} and those on Q^3 and Q^2 sites must have motional freedom that makes dipolar interactions weak. This supports rapid motions as the reason for long $T_{1\rho C}$ values of parent silica. Since all T_{dH} values are about 20-30 ms in TPM silica, all ^{1}H-^{1}H dipolar interactions in sample are about the same magnitude and

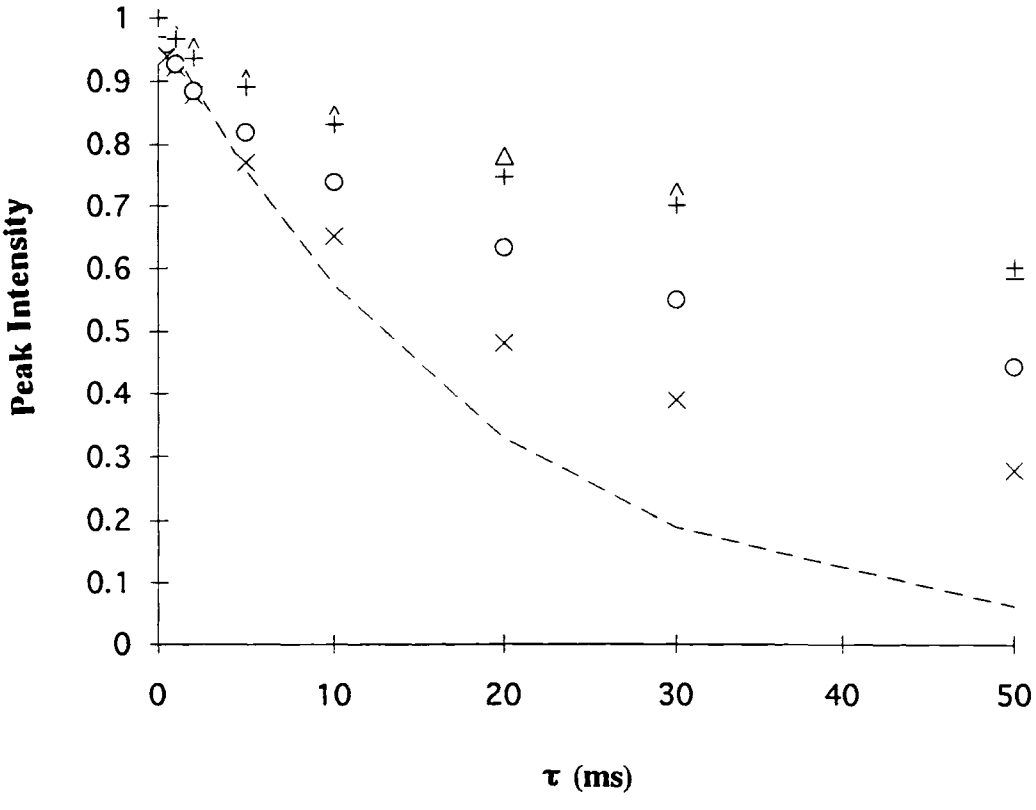

Figure 21. Plot of relaxation data in composite as a function of dalay time (τ). + = -C-, Δ = C=O, O = OCH$_3$, X= C-CH$_3$. The dashed line represents single exponential fit to the early data points for the α methyl carbon.

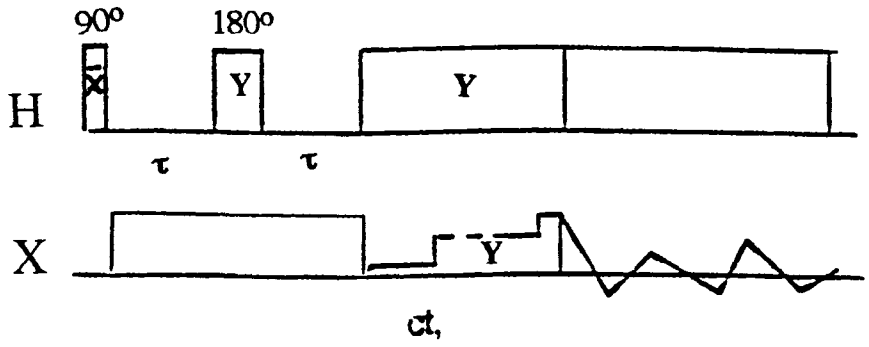

Figure 22. ^{1}H-^{1}H Dipolar dephasing pulse sequence

Table VII. Proton Dipolar Dephasing Time Constants (T_{dH}) in μs through ^{13}C and ^{29}Si Detection

Peaks	Parent Silica	TPM Silica	Composite	PMMA
		^{13}C Data[a]		
-C=O (PMMA)			7	8
-C=O (TPM)		29		
-C=		30		
$=CH_2$		65		
$-OCH_2$		36		
$-OCH_2CH_3$	24	21		
$-OCH_3$		25	8	8
-C-			7	8
$-Si-CH_2CH_2$		29		
$-C-CH_3$	30	33	9	8
$-Si-CH_2$		25		
		^{29}Si Data[a]		
Q^4	47	18	12	
Q^3	80	18	13	
Q^2	85	-	-	
S^3		25	9	
S^2		20	10	
S^1		21	9	

[a]Estimated error limits ± 10%.

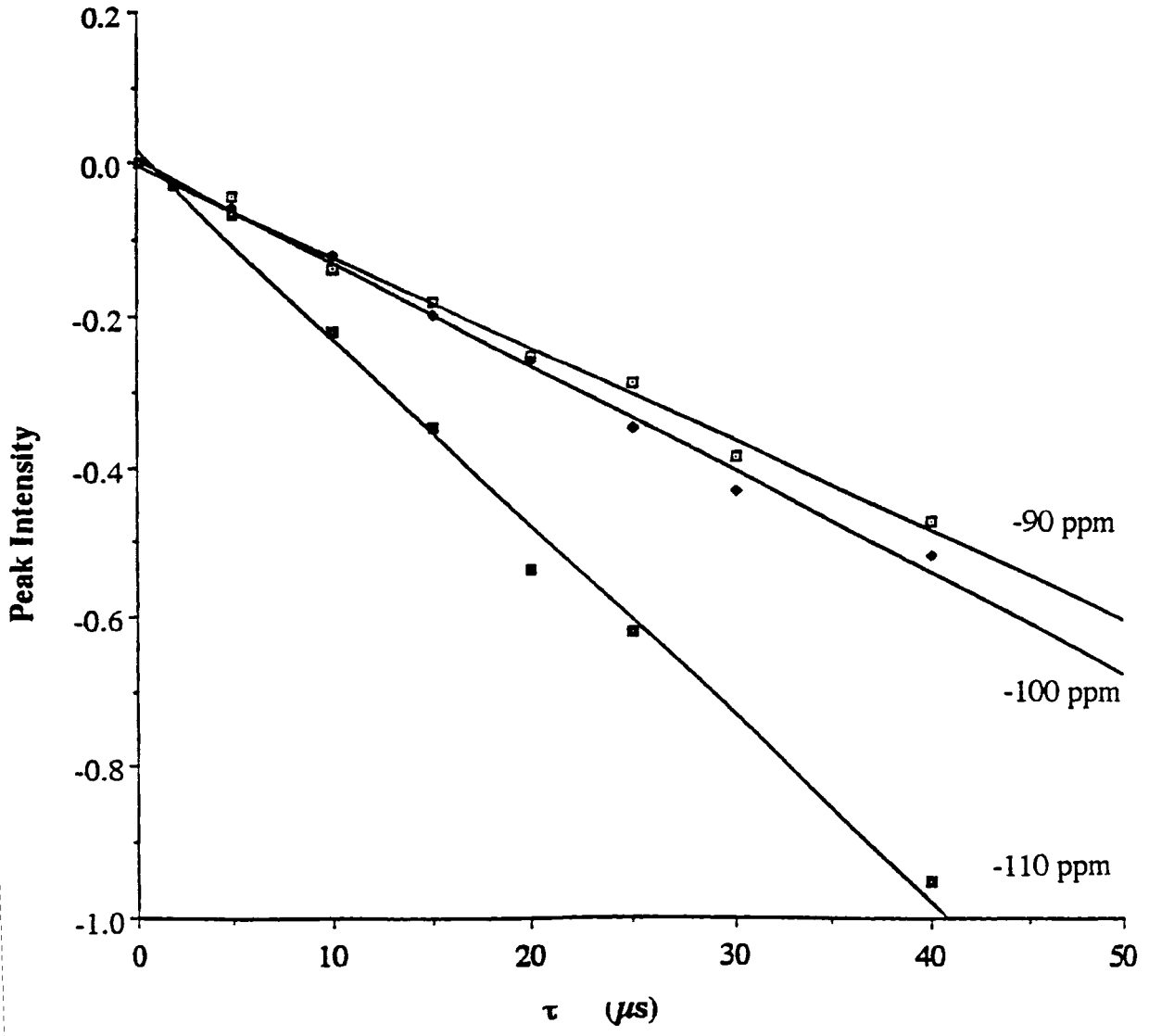

Figure 23. Semilog plot of magnetization versus delay time τ in μs for ^{29}Si of parent silica using the pulse sequence of Figure 21.

stronger than in parent silica. Still shorter T_{dH} in composite, and similar to that in PMMA, show that PMMA rigidifies the TPM layer.

Through ^{29}Si detection the protons coupled to Q^4 dephase at a faster rate than those coupled to Q^3 and Q^2. This means that the protons coupled to Q^4 Si atoms are more strongly dipolar coupled and dephase faster than the other protons in the system. Hence, during the dephasing period with increasing delay period their magnetization is attenuated, and on cross-polarization the Q^4 magnetization is developed at faster rate than Q^2 and Q^3 magnetization. This could be seen from a stack plot of the parent silica spectrum (Figure 24).

This accounts for the fast decay of Q^4 magnetization. Earlier in the chapter CPMAS studies had shown that the Q^4 sites that cross-polarize are close to the Q^3 sites (Table I). So it may be possible to say that the Q^3 silanols are involved in strong dipolar interactions are hydrogen-bonded. This supplements the observation of Maciel and co-workers,[9] in a proton CRAMPS study of a silica gel sample, that the silanol protons are involved in strong dipolar interactions are hydrogen bonded, as the silanol signal at 3.0-3.5 ppm attenuated after a 160 μs dipolar dephasing time. ^1H CRAMPS (Combined Rotation and Multiple Pulse Spectroscopy) studies are required to distinguish those interactions and are included in our future research plan.

Dipolar Dephasing and Spin Diffusion (SDDSH). This pulse sequence developed by Shanmin Zhang in our lab measures the ^1H spin-spin relaxation time constant T_2, as well as the rate of spin diffusion. The pulse sequence is given in Figure 25. Two equal pulses of opposite phase and variable duration τ enable measurement of the decay of the transverse magnetization as the time τ is increased. During the Y and $\overline{Y}$ pulses, the signal decays by proton-proton dipolar interactions. When the ^1H power is off, the signal decays by ^1H-^1H spin diffusion. The residual magnetization is allowed to

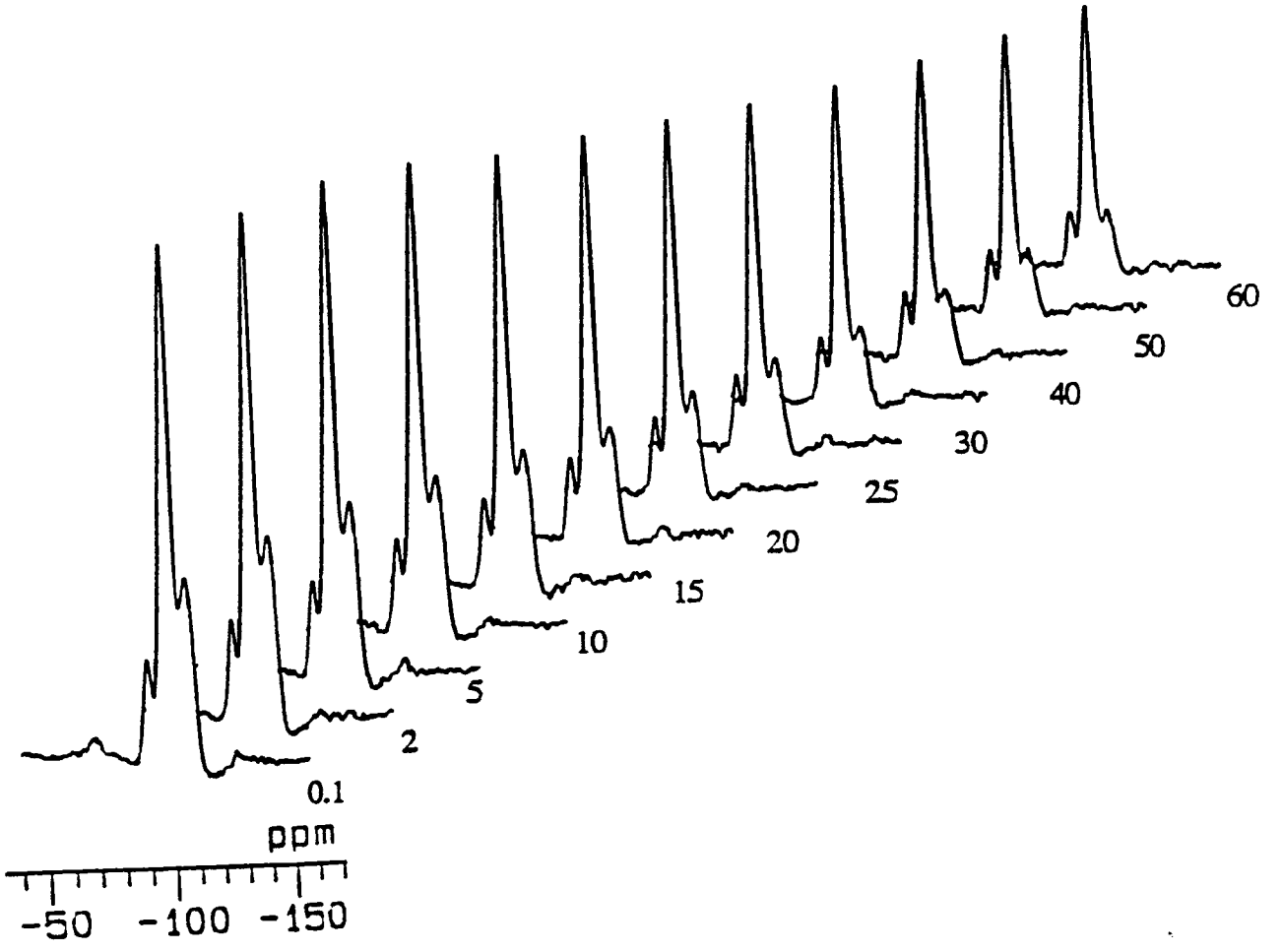

Figure 24. Stack plot of ^{29}Si parent silica SDDH relaxation measurements; 256 scans. The delay time τ is in microseconds.

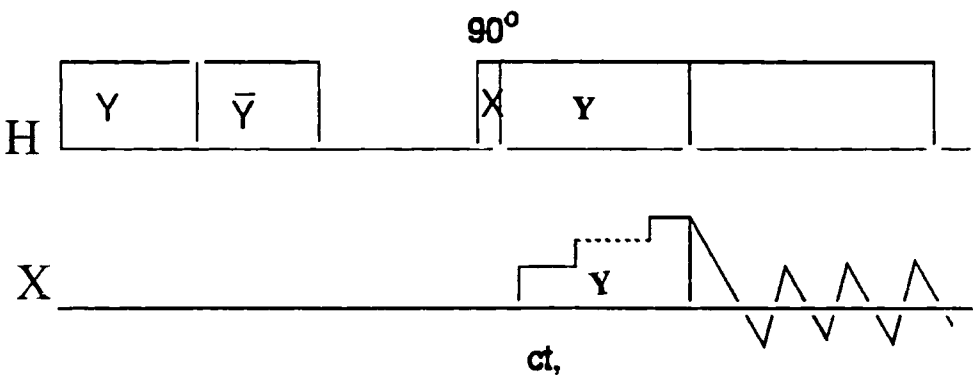

Figure 25. SDDSH pulse sequence. τ_1 is the mixing time in milliseconds.

equilibrate during a longer delay period τ_1 (1 ms), and the resulting X nucleus signal is generated by a QACP sequence.

This gives T_2, the spin-spin relaxation time constant, by fitting the experimental data to equation 6. The results from ^{29}Si detection are compiled in Table VIII. The values are found to decrease from the parent silica to the TPM silica to the least in the composite. This is expected as the systems are becoming more rigid. The observed trend has a T_2 cause. Without more detailed analysis, we cannot say how chemical shift dispersion contributes to the line widths.

In the second experiment the τ is kept constant and the equilibration time (τ_1) is varied. After the initial pulse period, the proton magnetization from different environments decays at different rates, due to the differences in spin-spin relaxation times. The magnetization that survives a particular time period is allowed to equilibrate during τ_1. The magnetization evolved is then detected through the QACP pulse sequence. The spin diffusion could be observed if the signal intensity varies as the equilibration time (τ_1) is varied.

To test the above phenomenon in parent silica, the τ value was kept constant at 7 μs (during this little decay of the transverse magnetization should have occurred), and the τ_1 values were varied. The plot of peak intensity (normalized with respect to the least τ_1) versus τ_1 is given for parent silica in Figure 26. No significant decrease or increase in the magnetization was observed, suggesting inefficient spin diffusion during the short delay period τ.

In another experiment the τ value was increased to 30 μs, allowing a clear distinction of the residual magnetization (Figure 27). The strongly dipolar coupled protons that cross-polarize Q^4 have now lost more of their magnetization by spin-spin relaxation than the weakly dipolar coupled ones that cross-polarize Q^2. During the

Table VIII. ^{1}H T_2 Values in μs through ^{29}Si Detection from Pulse Sequence of Figure 25[a]

Peaks	Parent Silica	TPM Silica	Composite
Q^4	78	48	35
Q^3	135	46	35
Q^2	148[b]	45	-
S^3		72	28
S^2		58	26
S^1		55	25

[a] Estimated error limits ± 10%. [b]Estimated error limit ± 15%.

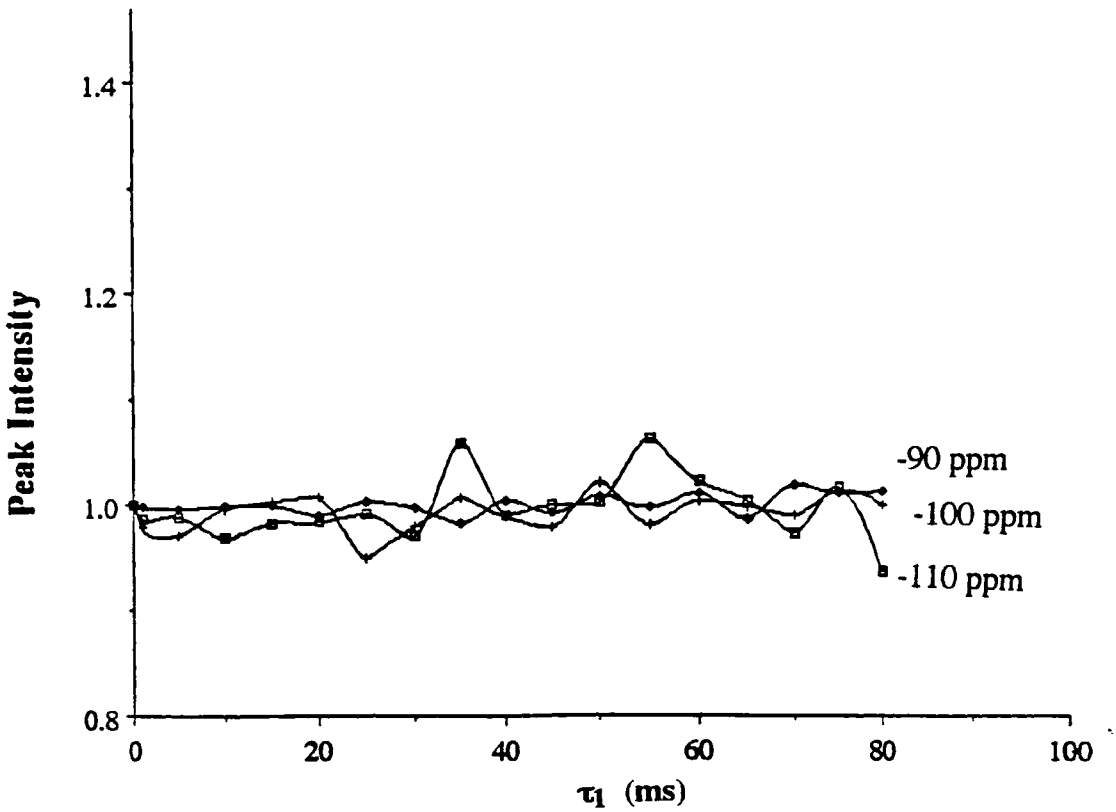

Figure 26. Relative change of magnetization of Q^2, Q^3, and Q^4 peaks in the parent silica sample obtained using the pulse sequence SDDSH (Figure 21) with variable τ_1 values in ^{29}Si mode; τ kept constant at 7 μs. Peak intensity is obtained by normalizing the magnetization with $\tau_1 = 0$.

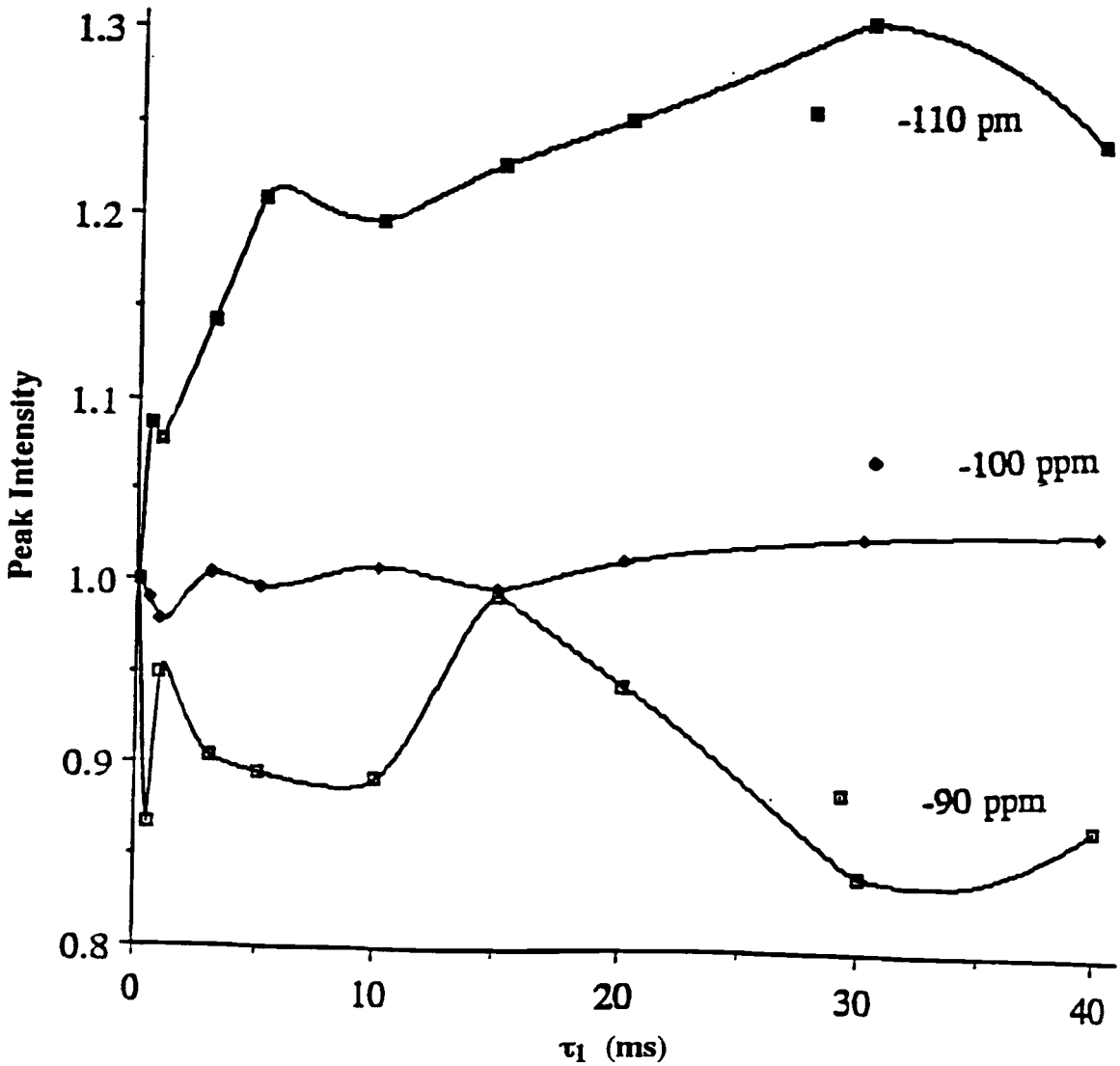

Figure 27. Relative change of magnetization of Q^2, Q^3, and Q^4peaks in the parent silica sample obtained using the pulse sequence SDDSH (Figure 21) with variable τ_1 values in ^{29}Si mode; τ kept constant at 30 μs. Peak intensity is obtained by normalizing the magnetization with $\tau_1 = 0$.

mixing time (τ_1) spin diffusion occurs by ^1H-^1H spin flip-flops, whereby the faster relaxing Q^4 sites gain magnetization from the slower relaxing Q^2 sites. This proves that there is spin diffusion between Q^2 and Q^4 sites. Direct proof of spin diffusion from Q^2-coupled protons to Q^4-coupled protons is in Figure 27.

Conclusions

Various pulse sequences were used to probe the interface between the TPM modified colloidal silica and the PMMA matrix in the TPM silica-PMMA composites. The quasi-adiabatic cross-polarization pulse sequence gave good signal-to-noise and well resolved ^{13}C and ^{29}Si spectra for the three samples. This enabled identification of various carbon and silicon environments in these samples. The ^{13}C CPMAS spectrum of the parent silica showed the presence of ethoxy groups remaining from TEOS used to synthesize the silica particles. Deconvolution of the ^{29}Si CPMAS spectra revealed that 78% of the Q^4 sites are not detected by cross-polarization. Those sites must not have Q^2 or Q^3 neighbors. The percentage contributions of the different Si atoms were elucidated from the deconvolution of the ^{29}Si single pulse spectra. The surface modifier TPM contributes about 22% to the total Si sites in the TPM silica and composite samples.

Identical T_{1H} values of 0.5-0.6 s obtained through detection of every ^{13}C and ^{29}Si signal reveal that magnetization of the protons in different environments equilibrates by spin diffusion in much less than 0.5 s. Similar $T_{1\rho H}$ values within each sample also suggest efficient spin diffusion. This proves that the PMMA is well mixed with the silica. The TPM silica in the PMMA matrix does not add rigidity to the composite, since the $T_{1\rho H}$ are found to be same for the composite and PMMA.

The ^1H-^1H dipolar dephasing study showed that the silanol protons are strongly dipolar coupled. And finally, the new pulse program (Figure 21) allows measurement of the proton spin-spin relaxation time (T_2) and proton spin diffusion from the same pulse program. Efficient spin diffusion has been observed between the Q^2 and Q^4 sites in the colloidal silica sample.

References

(1) Chuang, I-S.; Kinney, D. R.; Maciel, G. E. *J. Am.. Chem. Soc.* **1993**, *115*, 8695.

(2) Maciel, G. E.; Sindorf, D. W.; Bartuska, V. J. *J. Chromatogr.* **1981**, *205*, 438.

(3) Sindorf, D. W.; Maciel, G. E. *J. Am. Chem. Soc.* **1981**, *103*, 4263.

(4) Sindorf, D. W.; Maciel, G. E. *J. Am. Chem. Soc.* **1983**, *105*, 3767.

(5) Sindorf, D. W.; Maciel, G. E. *J. Phys. Chem.* **1983**, *87*, 5516.

(6) Sindorf, D. W.; Maciel, G. E. *J. Am. Chem. Soc.* **1983**, *105*, 1849.

(7) Maciel, G. E.; Sindorf, D. W. *J. Am. Chem. Soc.* **1980**, *102*, 7606.

(8) Sindorf, D. W.; Maciel, G. E. *J. Am. Chem. Soc.* **1983**, *105*, 1487.

(9) Bronnimann, C. E.; Zeigler, R. C.; Maciel, G. E. *J. Am. Chem. Soc.* **1988**, *110*, 2023.

(10) Chuang, I-S.; Kinney, D. R.; Bronnimann, C. E.; Ziegler, R. C.; Maciel, G. E. *J. Phys. Chem.* **1992**, *96*, 4027.

(11) Kinney, D. R.; Chuang, I-S.; Maciel, G. E. *J. Am. Chem. Soc.* **1993**, *115*, 6786.

(12) Rahman, A. *Nuclear Magnetic Resonance*; Springer-Verlag: New York, 1986.

(13) Hartmann, S. R.; Hahn, E. L. *Phys. Rev.* **1962**, *128*, 2042.

(14) Zhang, S.; Ford, W. T.; Czekaj, C. *J. Magn. Res. Ser. A.* **1994**, *111*, 87.

(15) Edzes, H. T. *Polymer* **1983**, *24*, 1425.

(16) Bogush, G. H.; Tracy, M. A.; Zukoski IV, C. F. *J. Non-Cryst. Solids* **1988**, *104*, 95.

(17) De Hann, J. W.; Van Den Bogaert, H. M.; Ponjee, J J.; Van De Ven, L. J. M; *J. Coll. Interface Sci.* **1986**, *110*, 591.

(18) Hair, M. L. In "*Chemically Modified Surfaces Vol. 1, Silane Surfaces and Interfaces*", Ed. Leyden, D. E. Gordon and Breach Science Publishers, New York 1986.

(19) Farrar, T. C.; Becker, E. D. *Pulse and Fourier Transform NMR, Introduction to Theory and Methods*, Acadamic Press: New York, 1971.

(20) Fukushima, E.; Roeder, S. B. W. *Experimental Pulse NMR, A Nuts and Bolts Approach*, Addison-Wesley Publishing Company, Inc.: Ontario, 1981.

(21) Huijgen, T. P.; Angad Gaur, H.; Weeding, T. L.; Jenneskens, L. W.; Schurs, H. E. C.; Huysmans, W. G. B.; Veeman, W. S. *Macromolecules* **1990**, *23*, 3063.

(22) Weeding, T. L.; Veeman, W. S.; Jenneskens, L. W.; Angad Gaur, H.;Schuurs, H. E. C.; Huysmans, W. G. B. *Macromolecules* **1989**, *22*, 706.

(23) Lauprêtre, F. In "*NMR Spectroscopy of Polymers*", Ed. Ibbett, R. N. Blackie Academic & Professional, New York, 1993.

(24) Schaefer, J.; Stejskal, E. O.; Buchdahl, R. *Macromolecules* **1977**, *10*, 384.

(25) Edzes, H. T.; Veeman, W. S. *Polym. Bull.* **1981**, *5*, 255.

VITA

Joseph Roychen

Candidate for the Degree of

Master of Science

Thesis: SOLID STATE NMR STUDY OF THE INTERFACIAL REGION IN SURFACE MODIFIED SILICA-POLY(METHYL METHACRYLATE) COMPOSITES

Major Field: Chemistry

Biographical:

Personal Data: Born in Kerala, India, March 1966, son of K. M. Joseph and Mary.

Education: Received Bachelor of Science Degree in Chemistry from Sardar Patel University in May, 1986; Master of Science in Industrial Polymer Chemistry from Sardar Patel University in May, 1988; Doctor of Philosophy in Chemistry from M. S. University of Baroda in December, 1992; completed requirements for the Master of Science Degree at Oklahoma State University in July, 1995.

Professional Experience: Teaching Assistant, Department of Chemistry, Oklahoma State University, August, 1992 to December, 1994; Research Assistant, Department of Chemistry, Oklahoma State University, January, 1995 to July, 1995.

Professional memberships: American Chemical Society.